The miR-155–PU.1 axis acts on Pax5 to enable efficient terminal B cell differentiation

Dong Lu,[1] Rinako Nakagawa,[1] Sandra Lazzaro,[1] Philipp Staudacher,[1] Cei Abreu-Goodger,[3] Tom Henley,[1] Sara Boiani,[1] Rebecca Leyland,[1] Alison Galloway,[1] Simon Andrews,[2] Geoffrey Butcher,[1] Stephen L. Nutt,[4,5] Martin Turner,[1] and Elena Vigorito[1]

[1]Lymphocyte Signaling and Development and [2]The Bioinformatics Group, The Babraham Institute, Babraham Research Campus, Cambridge, Cambridgeshire CB22 3AT, England, UK
[3]National Laboratory of Genomics for Biodiversity (Langbio), Cinvestav, Irapuato, 36821 Guanajuato, Mexico
[4]The Walter and Eliza Hall Institute of Medical Research, Parkville, Australia 3010, Australia
[5]Department of Medical Biology, University of Melbourne, Parkville, Victoria 3010, Australia

A single microRNA (miRNA) can regulate the expression of many genes, though the level of repression imparted on any given target is generally low. How then is the selective pressure for a single miRNA/target interaction maintained across long evolutionary distances? We addressed this problem by disrupting in vivo the interaction between miR-155 and PU.1 in mice. Remarkably, this interaction proved to be key to promoting optimal T cell–dependent B cell responses, a previously unrecognized role for PU.1. Mechanistically, miR-155 inhibits PU.1 expression, leading to Pax5 down-regulation and the initiation of the plasma cell differentiation pathway. Additional PU.1 targets include a network of genes whose products are involved in adhesion, with direct links to B–T cell interactions. We conclude that the evolutionary adaptive selection of the miR-155–PU.1 interaction is exercised through the effectiveness of terminal B cell differentiation.

CORRESPONDENCE
Martin Turner:
martin.turner@babraham.ac.uk
OR
Elena Vigorito:
elena.vigorito@babraham.ac.uk

Abbreviations used: ASC, antibody-secreting cells; ChIP, chromatin immunoprecipitation; CSR, class switch recombination; DEG, differentially expressed genes; GC, germinal center; miRNA, microRNA; RPKM, reads per transcript corrected per million mapped reads; Seq, sequencing; UTR, untranslated region.

The study of the regulatory networks that control cell fate decisions and developmental processes in mammals has mainly been focused on identifying the molecular components and their interactions, usually in a qualitative rather than a quantitative manner. A successful example of this approach is the well-characterized system of terminal differentiation of B cells, which allows study of the interconnected processes of cellular expansion, differentiation, and cell fate determination. Antigen-activated B cells receive additional signals from helper T cells before undergoing proliferative expansion. After a few rounds of division, some of the resulting B-blasts migrate to the extrafollicular regions in the spleen or to the medullary cords of lymph nodes, where they continue to proliferate before differentiating into antibody-secreting cells (ASCs; the term is used here to include cycling plasmablasts and plasma cells). This leads to the immediate production of neutralizing antibody that can be critical to the control of the spread of an infection as well as to the formation of immune complexes that assist antigen presentation (MacLennan et al., 2003; Belver et al., 2011). Such extrafollicular responses can involve antibody (Ab) class switch recombination (CSR) to various isotypes, allowing the Abs produced to acquire a wide range of effector functions and to disseminate toward infected tissues. Other B-blasts migrate to the B cell follicles, make cognate interactions with antigen-primed T cells and form germinal centers (GC). After accumulation of somatic mutations in their immunoglobulin genes, GC-B cells are subjected to antigen affinity-based selection. This process shapes the BCR repertoire of antigen experienced B cells by providing survival signals to non self-reactive, high affinity clones to become long-lived plasma cells or memory B cells (Ho et al., 1986; Jacob et al., 1991a; Liu et al., 1991).

B cell terminal differentiation is a particularly attractive system in which to study gene regulatory networks because of the well-defined gene expression changes that occur during the progression from naive B cells to ASCs and the

The Rockefeller University Press $30.00
J. Exp. Med. 2014 Vol. 211 No. 11 2183-2198
www.jem.org/cgi/doi/10.1084/jem.20140338

The Journal of Experimental Medicine

documented interactions between the major transcription factors involved. In qualitative terms, the changes in gene expression required for this process are regulated by the coordinated activity of transcription factors that either maintain the B cell program (Pax5, Bach2, and Bcl6) or promote differentiation (Blimp1 or IRF4; Martins and Calame, 2008). Interestingly, the abundance of these transcription factors is tightly regulated in specific windows along the pathway of terminal B cell differentiation. For instance, haploinsufficient Bcl6 B cells are less able to establish GC compared with their WT counterparts (Linterman et al., 2009). Thresholds of IRF4 direct different outcomes of B cell differentiation: whereas low expression of IRF4 promotes GC development and CSR and blocks the formation of ASCs, the opposite occurs when it is highly expressed (Sciammas et al., 2006; Ochiai et al., 2013). Thus, changes in the abundance of at least some components of the network may affect the outcome of the differentiation program. However, how thresholds and abundances are regulated in vivo is an issue that remains to be elucidated. This unresolved issue is of wide biological significance which has long been acknowledged in the context of many human developmental syndromes caused by partial, heterozygous chromosomal loss (Fisher and Scambler, 1994) and involving the deletion of critical haploinsufficient genes. Although those changes in gene expression can be limited in range (>1–2 fold), they dramatically impact developmental processes leading to cancer susceptibility and tumor formation (Berger and Pandolfi, 2011).

A major mechanism to enable stringent control of gene expression involves microRNAs (miRNAs), with most genes in the genome being predicted to be under their control (Friedman et al., 2009). However, the effect of a particular miRNA on a specific gene is generally limited to no more than a two- to threefold change in expression. An unsolved question in the miRNA field is what keeps miRNA-responding elements under strict evolutionary purifying selection, if they merely fine-tune the expression of their targets. We speculate that the small changes imparted by miRNA regulation, at the very least in certain network components, may make a substantial contribution to the efficiency of a particular biological process.

To shed some light on this problem, we assessed the impact on terminal B cell differentiation in vivo of disrupting a miRNA-responding element within the mRNA of a particular transcription factor. This approach, which directly prevents miRNA–target interactions, has rarely been used to investigate miRNA–target function (Dorsett et al., 2008), despite being the only way to establish causative relations. We chose the transcription factor PU.1 for several reasons. First, it is already established as a dose-sensitive gene. PU.1 functions in a concentration-dependent manner to regulate gene expression in many cell lineages (Laslo et al., 2006; Carotta et al., 2010a), and several animal models expressing variable amounts of PU.1 have altered hematopoiesis (Rosenbauer et al., 2004; Dakic et al., 2005; Iwasaki et al., 2005; Houston et al., 2007). Second, when overexpressed by means of retroviral transduction of mitogen- and cytokine-activated B lymphocytes, it is a negative regulator of CSR (Vigorito et al., 2007). Third, PU.1 expression in B cells is elevated in the absence of miR-155, a miRNA that regulates T cell–dependent antibody responses in a B cell intrinsic manner (Vigorito et al., 2007). Last, the role of PU.1 in terminal B cell differentiation is only beginning to be understood (Carotta et al., 2010b), so our investigation might yield valuable new insights into the mechanisms of this process.

By removing the miR-155–binding site in the 3′untranslated region (UTR) of PU.1 in mice, we uncoupled PU.1 expression from miR-155. This resulted in increased PU.1 levels in B cells. Remarkably, a twofold change in expression of PU.1 led to an impaired extrafollicular response to immunization in vivo and impaired CSR and plasma cell formation in cultured B cells. Mechanistically, we established that miR-155 is required for the initiation of the plasma cell differentiation program because it down-regulates PU.1, which in turn down-regulates Pax5. Furthermore, we uncovered a network of genes regulated by PU.1 with functions in cellular adhesion, suggesting that PU.1 controls B–T cell interactions. Our results also highlighted the fact that small changes in the expression of particular genes can have profound effects in regulatory networks and that tight control of their abundance by miRNAs is essential for optimal function.

RESULTS

Increased expression of PU.1 in activated B cells upon disruption of miR-155 regulation

To reveal the effect of altered PU.1 expression due to the removal of its regulation by miR-155, the highly conserved miR-155 recognition element in the 3′UTR of *Sfpi1*, which encodes PU.1, was mutated in mice (Fig. 1 A). The mutation disrupts the "seed-match," binding to miR-155 such that the repression by miR-155 is abolished (Fig. 1 B) without creating de novo seed-matches for any known miRNA reported in miRBase (Release 13.0, Sanger Institute). Mice were bred to produce homozygotes for the knock-in allele, which we termed PU.1^{155-}. PU.1$^{155-/155-}$ mice were born at normal frequencies within litters. As in miR-155$^{-/-}$ mice (Rodriguez et al., 2007), the proportions and numbers of developing and mature PU.1$^{155-/155-}$ lymphoid subsets and myeloid cells showed no differences relative to WT (Table 1). These results are consistent with the low expression of miR-155 in unstimulated cells (Thai et al., 2007; O'Connell et al., 2007).

To examine whether mutation of the miR-155–binding site in PU.1 altered its mRNA and protein expression, B cells were stimulated with LPS for 96 h in vitro, to induce expression of miR-155, before PU.1 expression was measured. Expression of PU.1 mRNA and protein was increased in both miR-155$^{-/-}$ and PU.1$^{155-/155-}$ B cells relative to WT controls (Fig. 1, C and D). The effect of miR-155 on PU.1 is specific to activated B cells, as the expression of PU.1 is equivalent in WT, PU.1$^{155-/155-}$, and miR-155$^{-/-}$ naive B cells (Fig. 4 B, PU.1) in developing B cells and in myeloid cells (Fig. 1 E). Moreover, the effect was restricted to PU.1 as another miR-155 target, AID (encoded by *Aicda*), was expressed at WT levels in

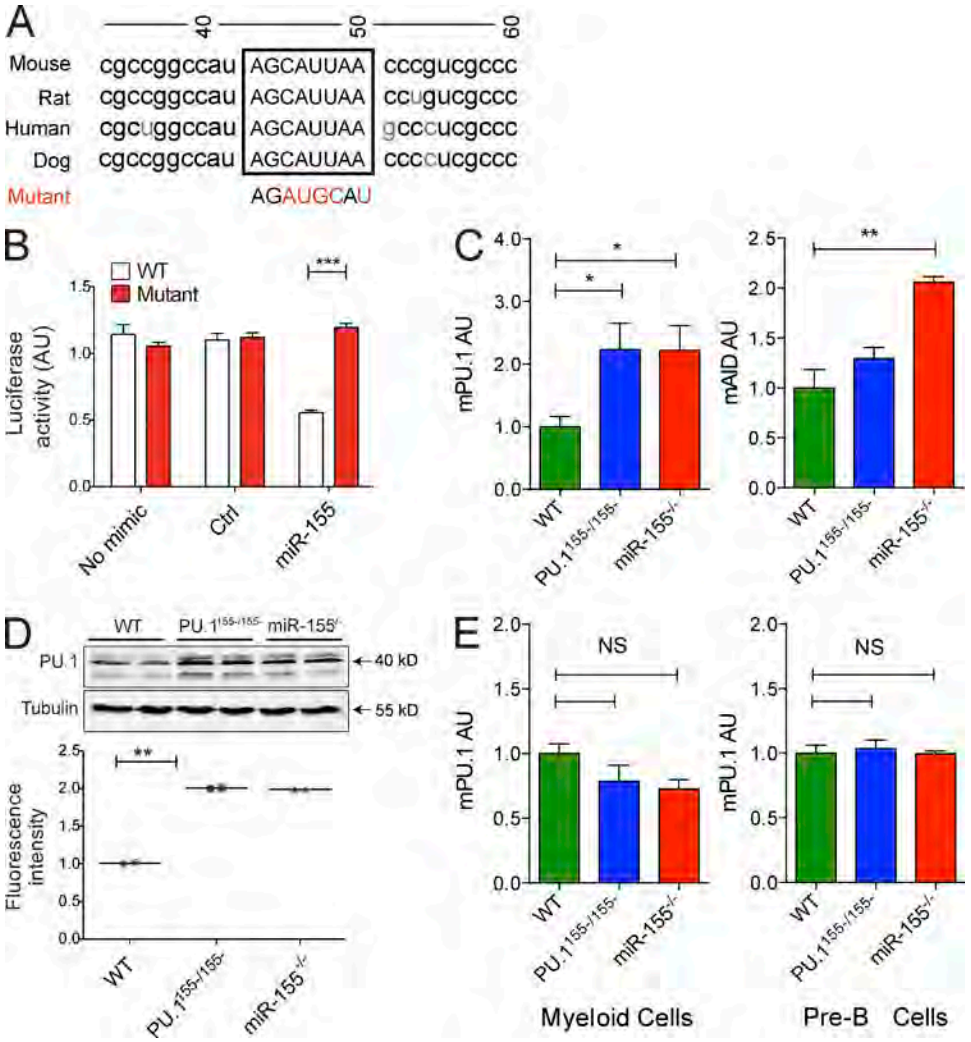

Figure 1. PU.1 expression is increased in activated B cells upon removal of the miR-155–binding site in its 3′UTR. (A) Schematic representation of a portion of the 3′UTR of the *Sfpi1* locus showing the conserved 8-nt seed complementary to miR-155 (boxed) and the base changes introduced to disrupt miR-155 binding (red letters). (B) A luciferase reporter assay was used to validate PU.1 as a direct target of miR-155 and to assess whether the mutation introduced in the 3′UTR of PU.1 disrupts miR-155 inhibition. WT (open bars) or mutant (filled [red] bars) plasmids containing the 3′UTR genomic region of PU.1 were amplified and co-transfected in triplicates with no mimic, control mimic (miR-124a), and miR-155 mimic into HeLa cells. The data presented correspond to the mean ± SEM from a representative experiment out of three. (C) Real-time PCR for PU.1 and AID expression in WT, $1^{155-/155-}$, and miR-155−/− B cells. Activation was achieved by stimulating cells with LPS and IL-4 for 4 d. Results are normalized against Hprt or β-actin expression and relative to the PU.1 and AID WT expression, respectively. Results are from three independent experiments with two to three mice per genotype per experiment. (D) Western blotting analysis of PU.1 in WT, PU.$1^{155-/155-}$, and miR-$155^{-/-}$ LPS-stimulated B cells for 4 d. Duplicate samples are shown with tubulin as loading control. Fluorescence intensity relative to WT is also shown. The results shown are representative of two experiments, with two mice per group. (E) Ex vivo pre-B cells ($B220^{low}$, IgM^-, $CD25^+$) and myeloid cells ($Gr\text{-}1^+/Mac\text{-}1^+$) from WT, PU.$1^{155-/155-}$, and miR-$155^{-/-}$ mice isolated from bone marrow by FACS sorting. PU.1 expression was measured by q-PCR using Hprt as control. Data represent the mean ± SEM from four mice per group. Statistical significance was assessed using one way ANOVA. *, P < 0.05; **, P < 0.001; ***, P < 0.0001. NS, not significant.

PU.$1^{155-/155-}$ B cells but up-regulated in miR-$155^{-/-}$ (Fig. 1 C). These data demonstrate that the binding site of miR-155 in the PU.1 3′UTR is functional and that miR-155 directly regulates the expression of PU.1 in activated B cells.

Impaired terminal B cell differentiation due to altered levels of PU.1 in vivo

Having established that miR-155 regulates the expression of PU.1 in activated B cells, we next studied the biological significance of this interaction in vivo. We took advantage of our previous observations with miR-$155^{-/-}$ mice in which we demonstrated a B cell–intrinsic defect in the T cell–dependent response to NP-KLH (Vigorito et al., 2007). We started by measuring the level of steady-state serum immunoglobulins IgM and IgG in the blood of PU.$1^{155-/155-}$ mice. We observed a significant reduction of serum IgM and IgG1 in PU.$1^{155-/155-}$ relative to WT mice (Fig. 2 A). A similar, though greater, effect was observed in miR-155–deficient mice. As

Table 1. Normal lymphoid and myeloid development in PU.1$^{155-/155-}$ mice

	No. of cells			Pax-5 (MFI)		
	WT	PU.1$^{155-/155-}$	miR-155$^{-/-}$	WT	PU.1$^{155-/155-}$	miR-155$^{-/-}$
Marrow						
Pre-pro[a]	$2 \times 10^5 \pm 1 \times 10^5$	$3.0 \times 10^6 \pm 5 \times 10^4$	$2.6 \times 10^5 \pm 8 \times 10^4$			
Pre B[b]	$1.8 \times 10^6 \pm 1 \times 10^5$	$2.9 \times 10^6 \pm 7 \times 10^5$	$2.2 \times 10^6 \pm 6 \times 10^5$	$2.2 \times 10^4 \pm 3 \times 10^3$	$2.4 \times 10^4 \pm 3 \times 10^3$	$2.3 \times 10^4 \pm 3 \times 10^3$
Immature B[c]	$9 \times 10^5 \pm 1 \times 10^5$	$1.2 \times 10^6 \pm 3 \times 10^5$	$9 \times 10^5 \pm 2 \times 10^5$	$2.8 \times 10^4 \pm 4 \times 10^3$	$3.0 \times 10^4 \pm 3 \times 10^3$	$3.0 \times 10^4 \pm 3 \times 10^3$
Mature B[d]	$9 \times 10^5 \pm 2 \times 10^5$	$1.2 \times 10^6 \pm 3 \times 10^5$	$1.1 \times 10^6 \pm 1 \times 10^5$	$1.2 \times 10^4 \pm 1 \times 10^3$	$1.3 \times 10^4 \pm 6 \times 10^2$	$1.3 \times 10^4 \pm 1 \times 10^3$
Myeloid[e]	$2.2 \times 10^7 \pm 5 \times 10^6$	$2.3 \times 10^7 \pm 2 \times 10^6$	$1.9 \times 10^7 \pm 3 \times 10^6$	$2.2 \times 10^4 \pm 3 \times 10^3$	$2.4 \times 10^4 \pm 3 \times 10^3$	$2.3 \times 10^4 \pm 3 \times 10^3$
Spleen				+++		
CD4 T	$2.9 \times 10^6 \pm 6 \times 10^5$	$2.5 \times 10^6 \pm 7 \times 10^5$	$2.7 \times 10^6 \pm 9 \times 10^5$			
CD8 T	$2.2 \times 10^6 \pm 9 \times 10^5$	$2.5 \times 10^6 \pm 1 \times 10^5$	$2.5 \times 10^6 \pm 8 \times 10^5$			
T1 B cells[f]	$5.1 \times 10^5 \pm 2 \times 10^5$	$4.8 \times 10^5 \pm 2 \times 10^5$	$8.3 \times 10^5 \pm 2 \times 10^5$	$1.7 \times 10^4 \pm 2 \times 10^2$	$1.6 \times 10^4 \pm 8 \times 10^2$	$1.6 \times 10^4 \pm 7 \times 10^2$
T2 B cells[g]	$4.9 \times 10^5 \pm 2 \times 10^5$	$5.3 \times 10^5 \pm 3 \times 10^5$	$7.0 \times 10^5 \pm 1 \times 10^5$	$1.7 \times 10^4 \pm 3 \times 10^2$	$1.5 \times 10^4 \pm 6 \times 10^2$	$1.5 \times 10^4 \pm 8 \times 10^2$
T3 B cells[h]	$2.7 \times 10^5 \pm 9 \times 10^4$	$2.7 \times 10^5 \pm 1 \times 10^5$	$3.4 \times 10^5 \pm 6 \times 10^4$	$1.4 \times 10^4 \pm 1 \times 10^3$	$1.3 \times 10^4 \pm 5 \times 10^2$	$1.3 \times 10^4 \pm 6 \times 10^2$
Fo B cells[i]	$1.6 \times 10^7 \pm 5 \times 10^6$	$1.6 \times 10^7 \pm 5 \times 10^6$	$1.7 \times 10^7 \pm 2 \times 10^6$	$9.5 \times 10^3 \pm 2 \times 10^2$	$8.8 \times 10^4 \pm 4 \times 10^2$	$8.6 \times 10^3 \pm 4 \times 10^2$
MZ B cells[j]	$8.7 \times 10^5 \pm 2 \times 10^5$	$7.4 \times 10^5 \pm 2 \times 10^5$	$1.4 \times 10^6 \pm 3 \times 10^5$	$1.4 \times 10^4 \pm 2 \times 10^2$	$1.2 \times 10^4 \pm 6 \times 10^2$	$1.2 \times 10^4 \pm 7 \times 10^2$
Myeloid cells[k]	$4 \times 10^6 \pm 1 \times 10^6$	$4 \times 10^6 \pm 1 \times 10^6$	$5 \times 10^6 \pm 1 \times 10^6$			
Peritoneal cavity						
B1a[l]	B1a [i]	$1.3 \times 10^5 \pm 5 \times 10^4$	$2 \times 10^5 \pm 1 \times 10^5$	$9.0 \times 10^3 \pm 9 \times 10^2$	$8.4 \times 10^3 \pm 6 \times 10^2$	$7.5 \times 10^3 \pm 7 \times 10^2$
B1b[m]	B1b [ii]	$7 \times 10^4 \pm 3 \times 10^4$	$9 \times 10^4 \pm 5 \times 10^4$	$8.2 \times 10^3 \pm 4 \times 10^2$	$8.1 \times 10^3 \pm 5 \times 10^2$	$7.5 \times 10^3 \pm 5 \times 10^2$
B2[n]	B2 [iii]	$1.6 \times 10^5 \pm 7 \times 10^4$	$5 \times 10^5 \pm 3 \times 10^5$	$8.4 \times 10^3 \pm 8 \times 10^2$	$8.5 \times 10^3 \pm 7 \times 10^2$	$7.7 \times 10^3 \pm 8 \times 10^2$
Myeloid[o]	Myeloid [iv]	$7 \times 10^5 \pm 4 \times 10^5$	$1.2 \times 10^6 \pm 8 \times 10^5$			

Data corresponds to mean and standard deviation from five mice each genotype. Data analysis in is based on one experiment with 4-5 biological replicates per genotype.

[a] B220$^{+/low}$, IgM$^-$ cKit$^+$
[b] B220^{low},IgM$^-$, CD25$^+$
[c] B220^{low},IgM$^+$
[d] B220+/IgM+
[e] Gr-1$^+$/Mac-1$^+$
[f] B220^{low},CD93$^+$, CD23^{low}, IgM^{high}
[g] B220^{low},CD93$^+$, CD23^{high}, IgM^{high}
[h] B220^{low},CD93$^+$, CD23^{high}, IgM^{low}.
[i] B220^{high},CD93$^-$, CD23$^+$, IgM$^+$
[j] B220^{high},CD93$^-$, CD23$^-$, IgM^{high}, CD21^{high}
[k] Gr-1$^+$/Mac-1$^+$
[l] CD5$^+$,Mac-1$^+$,B220^{low}
[m] CD5-,Mac-1$^+$,B220^{low}
[n] CD43^{low},Mac-1$^-$,B220^{low}
[o] Gr-1$^+$/Mac-1$^+$

the numbers of cells in the different B cell compartments (B1, B2, and marginal zone B cells) are not affected by changes in PU.1 abundance (Table 1), this result strongly suggests an activation defect. Therefore, we next measured the antigen-specific IgM and IgG1 responses to the immunogen NP-KLH in alum over time. At an early time point, day 7, we observed a decrease on antigen-specific antibody secretion in the PU.1$^{155-/155-}$ mice, although less severe than in the miR-155$^{-/-}$ mice, which was absent at later time points (Fig. 2 B and not depicted). These results suggest that miR-155 regulation of PU.1 is required for an optimal extrafollicular response but does not affect the GC output, suggesting the involvement of additional miR-155 targets in the context of the GC response. The early extrafollicular response is dominated by antibody production that is dependent on the rapid differentiation of proliferating B cells into IgM or IgG1 ASC located in secondary lymphoid organs (Jacob et al., 1991b). Quantitation of the number of NP-specific IgM or IgG1 ASCs in the spleen by ELISPOT at day 7 allows direct examination of the extrafollicular response. The number of NP-specific IgM ASC in PU.1$^{155-/155-}$ mice was reduced relative to WT mice to an extent similar to that in miR-155$^{-/-}$ mice (Fig. 2 C). However, NP-specific IgG1 ASC from PU.1$^{155-/155-}$ mice, although significantly reduced relative to WT, were not as severely impaired as in the miR-155$^{-/-}$ response (Fig. 2 C). We wished to determine whether the impaired antibody production in PU.1$^{155-/155-}$ mice was intrinsic to B cells. To this end, we created mixed chimeras by transferring 20% of WT, PPU.1$^{155-/155-}$, or miR-155–deficient bone marrow cells with 80% of μMT-mutated bone marrow cells into sublethally irradiated μMT mice, as previously described (Vigorito et al., 2007). The μMT mutation prevents the generation of B cells, so the B cells in the chimeras will be WT, PU.1$^{155-/155-}$, or miR-155 deficient. The 20/80 ratio favors reconstitution of all the other hemopoietic lineages from WT precursors. The three groups of chimeras had similar proportions and numbers of B, CD4$^+$, and CD8$^+$ T cells (unpublished data). Analysis of the extrafollicular response in the PU.1$^{155-/155-}$ and miR-155–deficient chimeras recapitulated the phenotype observed in the corresponding germline mice: specifically, reduced number of NP-specific IgM and IgG1 ASC in the spleen 7 d after immunization (Fig. 2 D). These results demonstrate a B cell–intrinsic requirement for down-regulation of PU.1 by miR-155 at the early stages of a T cell–dependent response. In summary, our results not only demonstrate that PU.1 is a functional target of miR-155 that regulates the output

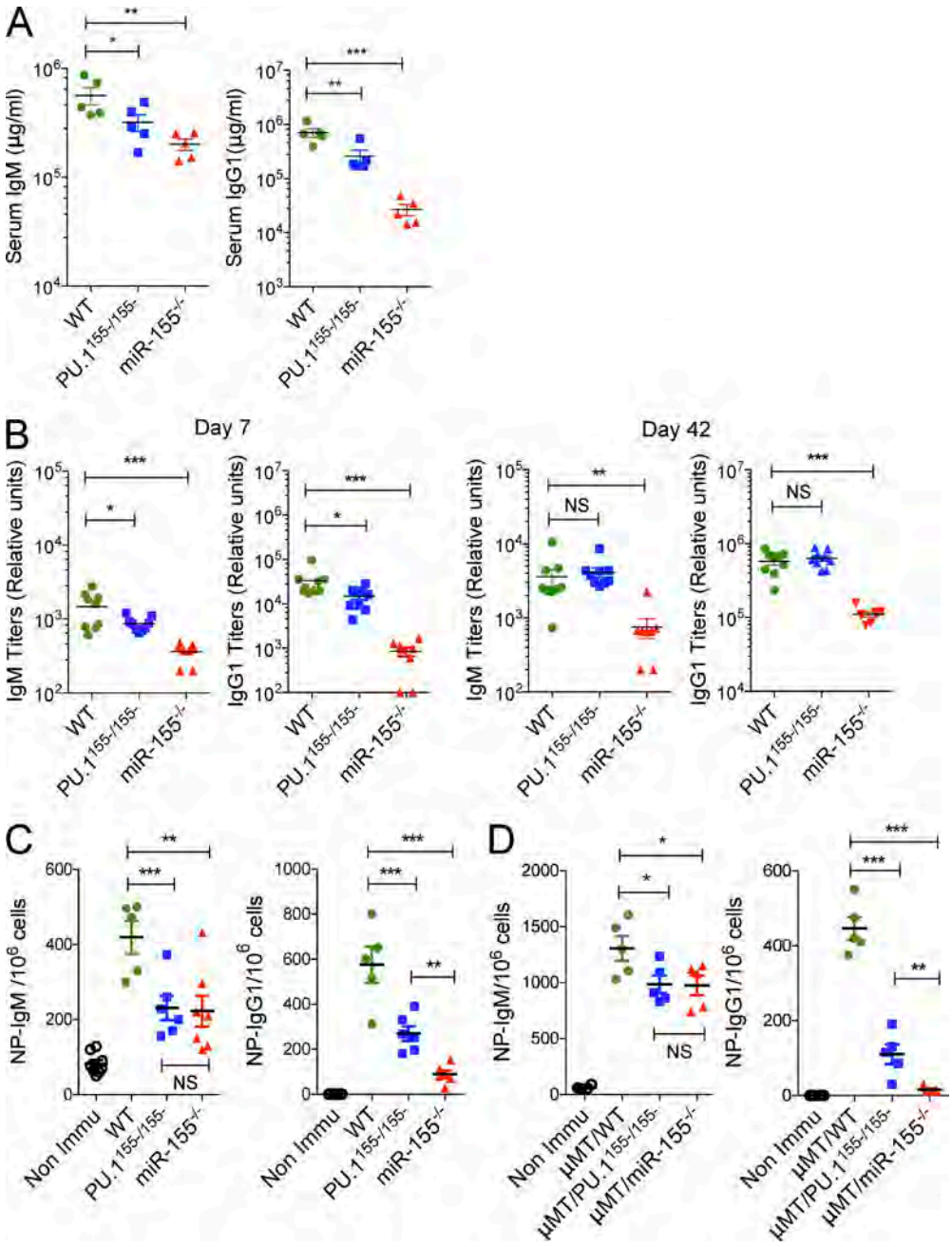

Figure 2. PU.1 is a negative regulator of Ig secretion in vivo. (A) Steady-state levels of serum IgM (left) and IgG1 (right) analyzed by ELISA. Each data point indicates IgM (left) or IgG1 (right) serum concentration (µg/ml) from one mouse. Horizontal bars correspond to the mean and the error bars to the SEM for the indicated genotype. The experiment was performed twice. (B) Titers of anti–NP-IgM and anti–NP-IgG1 were measured at 7 (left) or 42 d (right) after immunization with NP-KLH in alum. Data are present for 5–10 mice from 2 independent experiments. In all cases, each symbol represents one mouse. (C) ELISPOT analysis of splenic NP-specific IgM- (left) or IgG1-secreting cells (right) at day 7 after immunization with NP-KLH in alum. Data points indicate NP-specific cells per million cells and are presented as mean ± SEM from three different experiments, with three to five mice per genotype per experiment. (D) Similar to C, except that the experiment was performed with µMT/WT, µMT/PU.1$^{155-/155-}$, and µMT/miR-155$^{-/-}$ chimeras. In this experiment, 5 chimeric mice per group were used. Statistical analysis was assessed with two-sided ANOVA test. *, $P < 0.05$; **, $P < 0.001$; ***, $P < 0.0001$. NS, not significant.

of the extrafollicular response but also uncover a novel inhibitory role of PU.1 in terminal B cell differentiation in vivo. Our results also suggest that the amount of PU.1 is under stringent control in vivo, and small changes in its expression, due to miRNA regulation, affect adaptive immune responses.

Impaired plasma cell differentiation in activated PU.1$^{155-/155-}$ B cells correlates with increased expression of Pax5

To assess CSR and plasma cell differentiation independently of cell proliferation (Hasbold et al., 2004), we labeled B cells

with 5-(6) CFSE and examined cell surface expression of IgG1 and CD138 (a marker of plasmablasts and plasma cells) by flow cytometry over a time course of 5 d after stimulation with LPS and IL4. Cell division in PU.1$^{155-/155-}$ B cells was not different from that in WT B cells (Fig. 3, A and C). It was also not grossly affected in miR-155$^{-/-}$ B cells, as shown here (Fig. 3, A and C) and in previous studies (Thai et al., 2007; Dorsett et al., 2008; Teng et al., 2008). In contrast, CSR and plasma cell differentiation were significantly reduced both in PU.1$^{155-/155-}$ and miR-155–deficient B cells at all time points examined (Fig. 3 B). These observations suggest a developmental defect independent of cell cycle. Consistent with this, we previously showed intact post-switch circle transcription in miR-155$^{-/-}$ B cells compared with WT (Vigorito et al., 2007). Disruption of the miR-155–binding site in *Aicda* results in enhanced class switching by B cells (Dorsett et al., 2008; Teng et al., 2008), indicating that other miR-155 targets, unlike PU.1, are enhancers of class switching. Our results establish PU.1 as a consequential target of miR-155 that inhibits CSR and plasma cell differentiation.

Conditional deletion of Blimp1 in B cells has revealed that the plasma cell differentiation program is initiated by down-regulation of Pax5, which is followed by up-regulation of Blimp1 (Kallies et al., 2007), although it is still unclear how down-regulation of Pax5 is achieved. Expression of Pax5 in B cells is dependent on a promoter region regulated by EBF1 and a potent enhancer in its intron 5 (Decker et al., 2009). Interestingly, in early B cell development, the activity of this enhancer is regulated by the transcription factors PU.1, IRF4, IRF8, and NF-κB (Decker et al., 2009). We therefore hypothesized that the inhibitory effect of PU.1 on plasma cell differentiation is caused by a failure of PU.1$^{155-/155-}$ B cells to down-regulate Pax5. We first tested whether PU.1 binding to the Pax5 enhancer is detectable in activated B cells and whether that binding is affected by PU.1 abundance. To this end, we performed PU.1 chromatin immunoprecipitation (ChIP) followed by q-PCR to amplify the Pax5 enhancer element. We observed an increase in PU.1 binding in PU.1$^{155-/155-}$ and miR-155$^{-/-}$ B cells relative to WT levels (Fig. 4 A). Next, we looked at Pax5 mRNA and protein to determine whether PU.1 abundance, dependent on miR-155 regulation, may be having an impact on Pax5 expression. We sorted undifferentiated day 4 cultured B cells on the basis of being B220^{+}, IgG1^{-}, and CD138^{-}, and then measured their expression of Pax5. Our results show that both Pax5 mRNA and protein levels were increased in PU.1$^{155-/155-}$ and miR-155$^{-/-}$ B cells relative to WT (Fig. 4 B and not depicted), suggesting that this increase precedes plasma cell differentiation and is not affected by it. Consistent with defective plasma cell differentiation, the expression of Blimp1 was lower in PU.1$^{155-/155-}$ and miR-155$^{-/-}$ relative to WT levels (Fig. 4 B). Kinetic analysis showed that expression of PU.1,

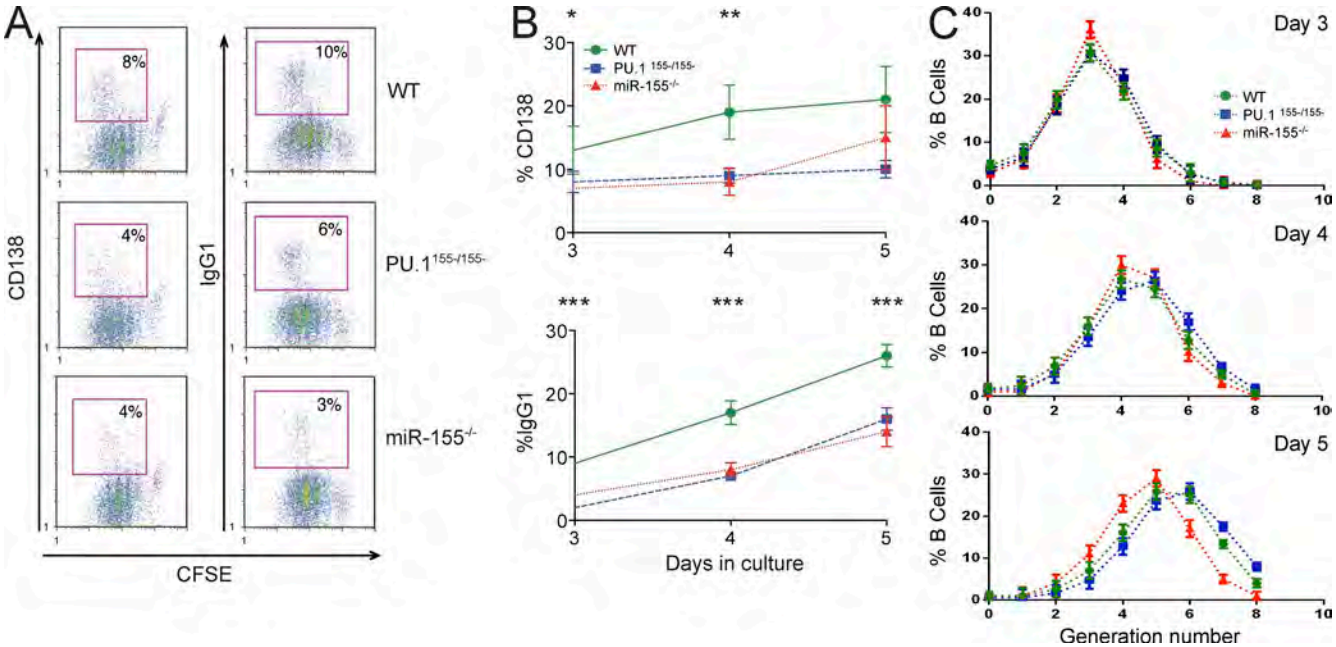

Figure 3. miR-155 down-regulation of PU.1 controls terminal B cell differentiation. (A) Typical FACS analysis profiles of splenic B220^{+} cells gated for either IgG1 or CD138 plasma cells after culture with LPS and IL-4 for 3 d. These are representative examples from three experiments, each with three mice per genotype. (B) Kinetics of LPS/IL-4 activation of WT, PU.1$^{155-/155-}$, and miR-155$^{-/-}$ B cells. Values presented are percentages of IgG1^{+} or CD138^{+} cells within the B220^{+} population. Results are presented as mean ± SD from three experiments with at least three mice of each genotype per experiment. (C) Splenic B cells of the indicated genotypes were CFSE labeled, followed by stimulation with LPS and IL-4. At the indicated time points, proliferation was assessed based on CFSE dilution using FlowJo. The graphs show the percentage of B cells in each generation. Symbols correspond to the mean and SEM for three mice, and it is a representative example from three experiments, each with three mice per genotype. Statistical analysis was assessed with one-way ANOVA test. *, $P < 0.05$; **, $P < 0.001$; ***, $P < 0.0001$.

Pax5, and Blimp-1 is equivalent in naive B cells from WT, PU.1$^{155-/155-}$, and miR-155$^{-/-}$ mice. This result is consistent with the equivalent levels of Pax5 that we observed in developing and mature naive B cell populations (Table 1), further reinforcing the view that miR-155 regulation of PU.1 is specific to activated B cells. The earliest change observed was the up-regulation of miR-155 in WT and PU.1$^{155-/155-}$ B cells and of PU.1 in PU.1$^{155-/155-}$ and miR-155$^{-/-}$ B cells, relative to WT, starting at day 1 of in vitro activation, followed by an increase in Pax5 and a decrease in Blimp-1 from day 3 (Fig. 4 B). Expression of Pax5 at day 3 suggests a slight delay in its up-regulation in PU.1$^{155-/155-}$ B cells relative to miR-155$^{-/-}$ (Fig. 4 B). We do not know the basis for this difference but it does not impact on Blimp-1 levels, which remain equivalent in

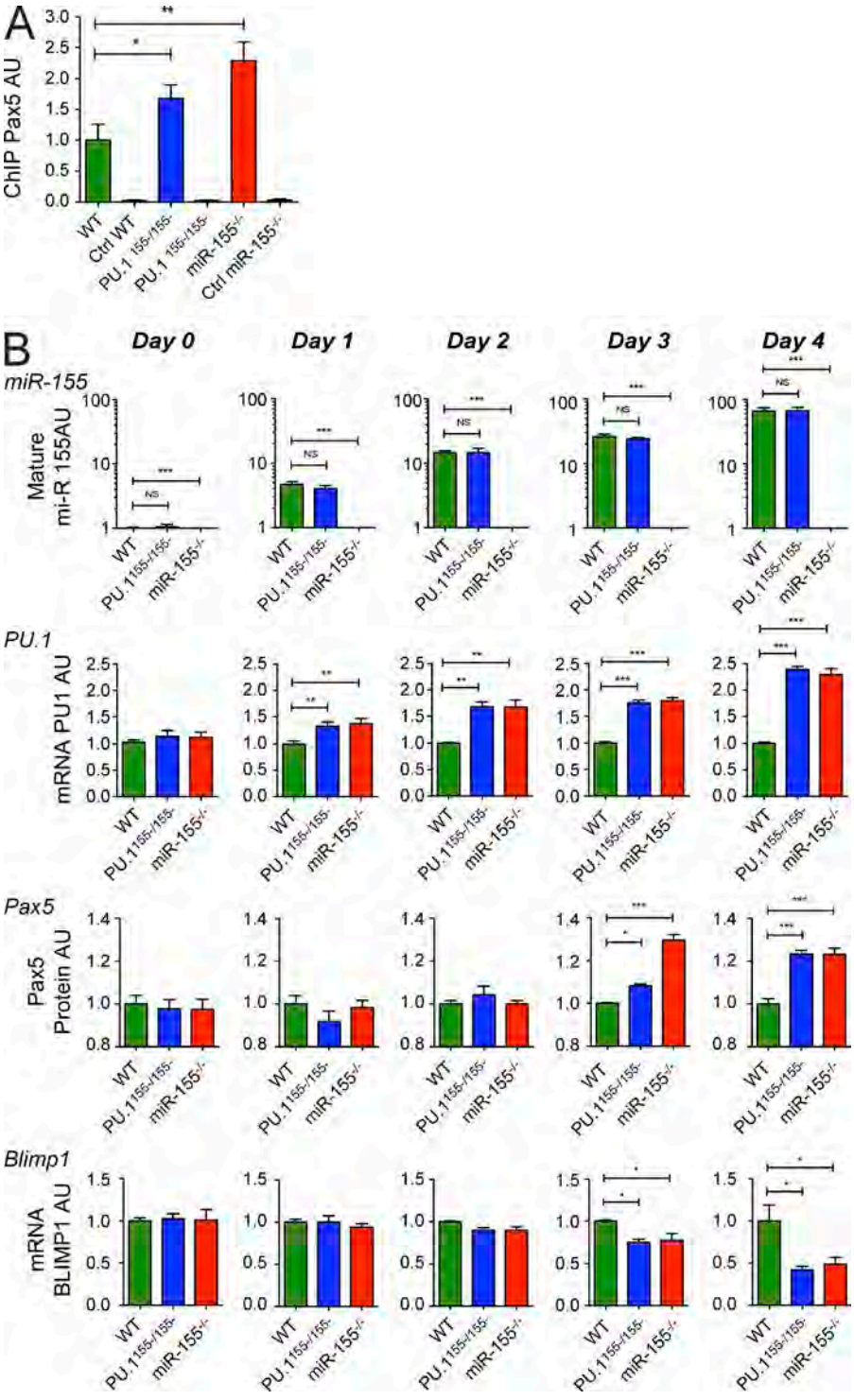

Figure 4. PU.1 down-regulation by miR-155 controls Pax5 and Blimp1 expression in activated B cells. (A) PU.1 binding to an enhancer regulatory element in intron 5 of Pax5. WT, PU.1$^{155-/155-}$, and miR-155$^{-/-}$ B cells were cultured with LPS and IL-4 for 4 d and ChIP was performed using rabbit α-PU.1 antibody or an isotype control antibody. Subsequently, real-time PCR was conducted to amplify a region in the enhancer element in intron 5 of Pax5 and data were normalized against β-actin. Data shown are fold change relative to WT percentage of input. Numbers represent the mean ± SEM from four independent experiments. (B) B cells from four mice of each genotype were cultured with LPS and IL-4 for the indicated times. miR-155 was measured using U6 as reference and its expression was calculated relative to ex vivo WT B cells. No expression was detected in miR-155$^{-/-}$ B cells. PU.1 and Blimp1 were measured by q-PCR using Hprt as control, whereas Pax5 expression was measured by flow cytometry. To facilitate the comparison to WT cells, expression at each time point is normalized to the WT control. Results are from two to three independent experiments, each with three to four mice per genotype. Statistical analysis was assessed with one-way ANOVA test. *, $P < 0.05$; **, $P < 0.001$; ***, $P < 0.0001$.

the two genotypes. We propose that in activated B cells, miR-155 down-regulates Pax5 by inhibiting PU.1 expression.

The plasma cell differentiation defect in PU.1$^{155-/155-}$-activated B cells can be rescued via forced reduction of Pax5 expression

To further elucidate the functional relationship between miR-155, PU.1, and Pax5, we tested whether reduction of Pax5 in PU.1$^{155-/155-}$ and miR-155$^{-/-}$ B cells would restore plasma cell differentiation without affecting WT B cells. To this end, we retrovirally transduced 24 h [LPS+IL-4]-activated B-blasts with a Pax5 silencing construct, and examined plasma cell and CSR 96 h later. Infected cells were monitored by expression of GFP from an IRES. Analysis of GFP$^+$ cells from control (empty vector)-transduced cells reproduced the plasma cell differentiation defect already described. However, silencing Pax5 specifically in PU.1$^{155-/155-}$ and miR-155$^{-/-}$ B cells reverted the phenotype, whereas it did not affect WT B cells (Fig. 5, A and B). The reversion was restricted to the GFP$^+$ fraction, consistent with a specific effect on Pax5 expression (Fig. 5, A and B). Moreover, CSR was unaffected by Pax5 silencing in all genotypes analyzed (unpublished data). Importantly, the extent of Pax5 reduction was similar in the three genotypes analyzed (Fig. 5 C). Collectively, our results suggest that regulation of Pax5 by the miR-155–PU.1 axis is an important step in B cells optimally differentiating toward plasma cells.

PU.1 target genes are enriched in genes encoding Ig superfamily proteins that regulate humoral responses in activated B cells

Having established that terminal B cell differentiation is sensitive to changes in PU.1 expression imparted by miR-155, we next assessed the impact of PU.1 on the gene expression program of activated B cells. After showing that plasma cell differentiation is sensitive to PU.1 levels, as an effect of elevated Pax5 expression, we turned our attention to CSR. To this end, we used culture conditions including LPS and a high concentration of IL-4, with the goal of identifying direct PU.1 targets important for this process. To identify direct target genes that respond to physiological changes in PU.1 concentration in activated B cells, we conducted chromatin immunoprecipitation coupled to deep sequencing (ChIP-Seq) from WT, PU.1$^{155-/155-}$, and miR-155$^{-/-}$-activated B cells. These results were combined with RNA deep sequencing (RNA-Seq) from the same samples. We predicted that genes that are differentially expressed in both PU.1$^{155-/155-}$ and miR-155$^{-/-}$ relative to WT might explain the CSR phenotype.

Our ChIP-Seq analysis identified 7,276 PU.1-bound genomic regions across the three genotypes. We next sought to identify genes expressed in B cells that were targeted by PU.1. To this end, we assigned peaks to annotated gene loci if peaks were within the gene body or up to ±50 kb beyond the gene. We defined as "expressed" genes whose expression is on average ≥1 RPKM (reads per kilobase per million mapped reads) in at least one of the three genotypes. We found that 72% of the PU.1 peaks we assigned to expressed genes overlapped with previously reported peaks in naive B cells (Heinz et al., 2010), though the total number of genomic regions with PU.1 binding in activated B cells was lower than in naive B cells. Nonetheless, similar to what has been seen in naive B cells, PU.1 binding in our activated B cells was mostly detected at intra- or intergenic regions remote from the transcription start site (TSS; unpublished data). Close to the TSS, a small percentage of binding events are clustered in expressed genes (8%) and in the up-regulated genes (7%), with little binding in the nonexpressed or down-regulated genes (unpublished data). We next examined enriched sequence elements to uncover the sequence determinants for PU.1 binding in activated B cells. The most enriched motifs, based on de novo motif analysis, were very similar between the promoter-proximal and -distal regions and resembled the known PU.1 consensus elements AAAGAGGAAGTG (PU.1), GGAAGT (PU.1 core), and GGAAGTGAAACT (PU.1:IRF composite; Heinz et al., 2010; unpublished data). In expressed genes, 73% of all PU.1-binding sites contain a PU.1 or ETS core motif, suggesting that PU.1 binds directly to a large fraction of its target sites (Fig. 6 A).

Interestingly, the probability of a gene being associated with a PU.1 peak increases sharply between the set of nonexpressed genes and the set of differentially expressed genes (DEGs) across the three genotypes. Thus, whereas only 1 in 8 of the nonexpressed genes was associated with a PU.1 peak, the frequency increased to 1 in 5 for the expressed genes and even further, to 1 in 3.5, for the DEGs (Fig. 6 B). Moreover, the presence of a PU.1/IRF or PU.1 binding motif within peaks follows a similar trend: ∼50% of the peaks associated with nonexpressed genes contain the motif, compared with 73 and 83% of the expressed genes and DEGs, respectively (Fig. 6 A and not depicted). However, the frequency of the different PU.1 motifs (PU.1, PU.1 core, and PU.1/IRF composite) was similar in expressed genes and DEGs (unpublished data). The enrichment in the proportion of genes associated with peaks concomitant with the enrichment in the presence of a recognized PU.1 binding motif in the set of DEGs, suggests this group of genes is enriched in direct PU.1 targets. Of note, the proportion of overlapping peaks in PU.1$^{155-/155-}$ and miR-155$^{-/-}$ was 89% in DEGs (Table S1).

We next examined the functional characterization of the group of genes differentially regulated in both PU.1$^{155-/155-}$ and miR-155$^{-/-}$ genotypes relative to WT B cells that are direct targets of PU.1 (119 genes, Table S1). Of these genes, 83% contained PU.1 binding motifs and, for 90% of them, PU.1 occupancy in naive B cells had been reported previously (Heinz et al., 2010), validating our results. The expression of *Prdm1* and *Syndican1* measured by RNA-Seq was within the background level for all genotypes, arguing against plasma cell differentiation taking place in these cultures (unpublished data). To determine the potential functional role of these gene expression changes, we looked for gene ontology (GO) biological processes significantly enriched in the list of DEGs that were also direct targets of PU.1. One of the highly ranked categories was "immunoglobulin subtype"

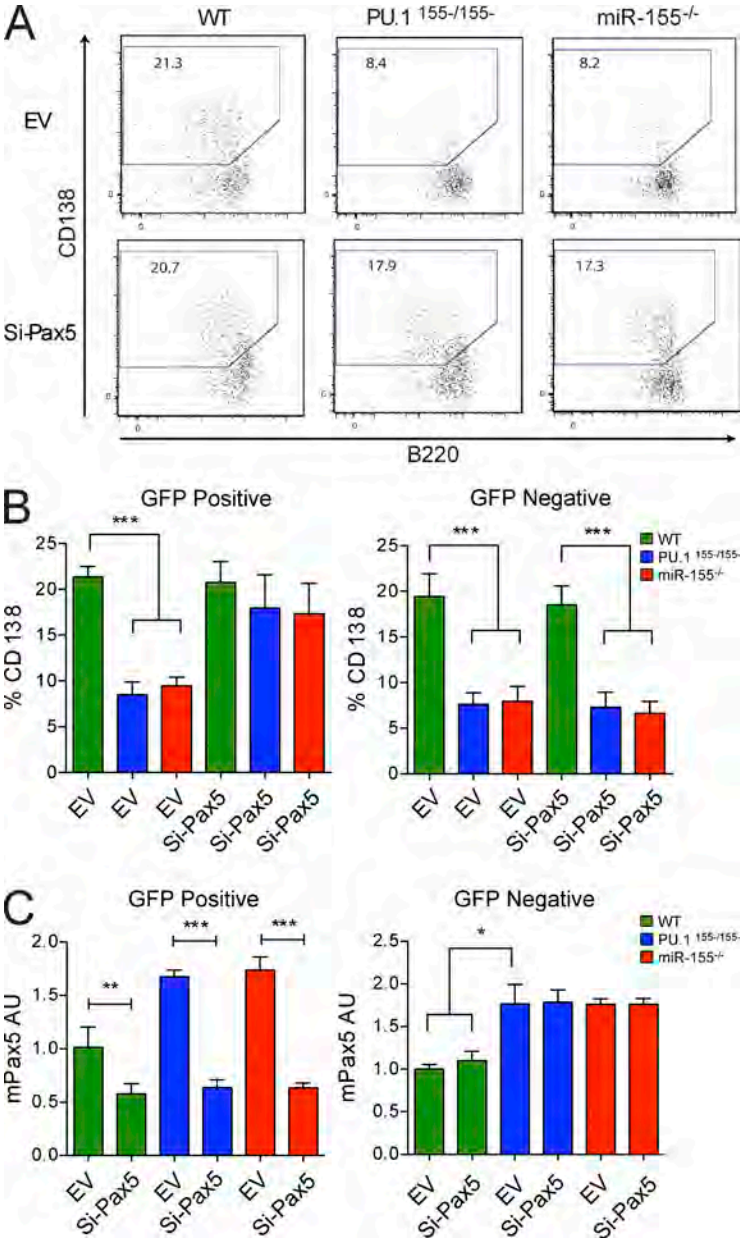

Figure 5. Forced reduction of Pax5 expression rescues the plasma cell differentiation defect in PU.1$^{155-/155-}$ and miR-155$^{-/-}$–activated B cells. (A) Representative plots of the CD138 and B220 expression levels in the WT, PU.1$^{155-/155-}$, and miR-155$^{-/-}$ activated B cells after transduction with GFP containing Si-Pax5 or empty control (EV) vector retroviruses. Cells were activated for 24 h before addition of the retroviruses, and were then cultured in activation media for an additional 3 d. The GFP$^+$ populations were selected for analysis. The numbers inside the gating boxes show the average percentage of gated population from a representative experiment out of three. (B) The bar graphs indicate the percentages of CD138-expressing cells among GFP$^+$ or GFP$^-$ gated populations. Data are aggregated from three independent experiments with three to four mice per group. (C) The Si-Pax5– or EV-transduced cells were sorted and gene silencing efficiencies in the WT, PU.1$^{155-/155-}$, and miR-155$^{-/-}$ samples were evaluated by qPCR. Bar graphs represent the mean from four independent experiments on either GFP$^+$ or GFP$^-$ populations. Statistical analysis was assessed with one-way ANOVA test. *, $P < 0.05$; **, $P < 0.001$; ***, $P < 0.0001$.

($P < 1.6 \times 10^{-5}$; unpublished data). Moreover, using ingenuity pathways analysis, which combines gene ontology categories and curated literature, one of the top processes was "humoral immune responses: production of antibodies" ($P < 6.8 \times 10^{-9}$; Fig. 6 C). This analysis led to the identification of ~30 PU.1 target genes with known links to humoral immune responses (Fig. 6 C and Table S1). The associated PU.1 binding and mRNA expression for some of the targets are shown in Fig. 6 (D and E). Similar patterns of expression were observed by RNA-Seq and quantitative PCR for 8 out of 9 validated genes (Fig. 6 E and not depicted).

Notably, 50% of these genes (Fig. 6 C, in red) encode members of the Ig superfamily of polypeptides, suggesting that PU.1 regulates genes involved in cellular adhesion and protein–protein interactions, critical processes in the context of T cell–dependent responses. Genes whose products are known to be important for sustaining interactions with T cells include *Icosl*, *Pvrl1*, *Pd1d1l2*, and *Slamf1*, although intrinsic roles in B cells for some of them remain to be assessed. Semaphorins (*Sema 7a*, *Sema 4a*, and *Cd300lf*), the semaphorin ligand Plexin-d1 (*Plxnd1*), and Fc-receptor genes (*FcgRIIb*, *FcgRIV*, and *Fcrl5*) are affected by PU.1 abundance. Proteins encoded by another group within the PU.1 targets are important in signal transduction downstream of some of the aforementioned receptors or the B cell receptor (*Dap12*, *Rasgrp3*, *Gab2*, and *Card11*). We also found that *Ccr7* and *Cxcr4*, which have known roles in the migration of activated B cells, are regulated by PU.1. Furthermore, most of the genes we identified

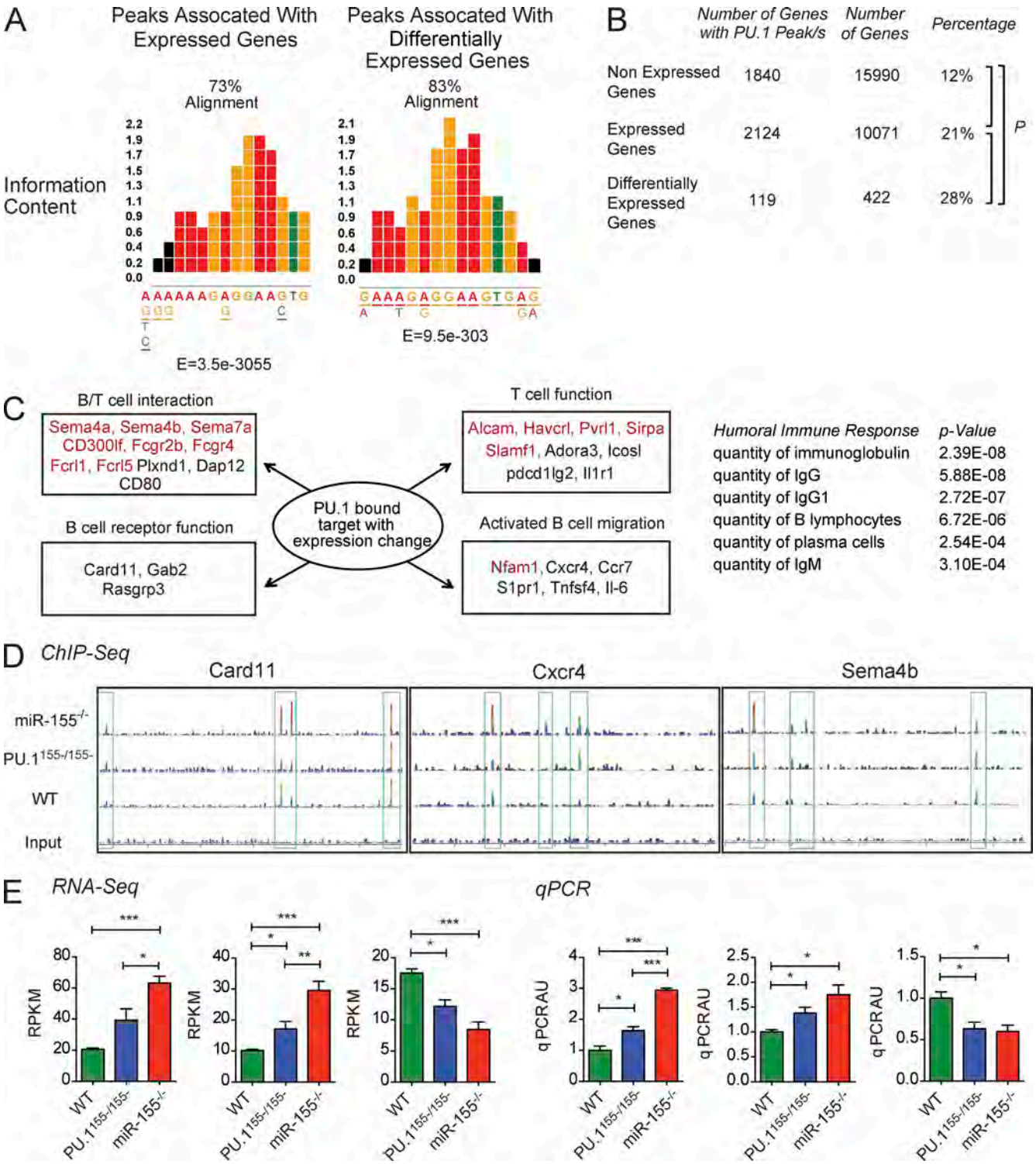

Figure 6. PU.1 targets in activated B cells include genes involved in adhesion and B/T cellular interactions. (A) A large proportion of DEGs bind PU.1 through its canonical site. The PU.1 motif was discovered using MEME (The MEME Suite), by alignment of the center (core 200 bp) of the PU.1 ChIP-peaks in either DEGs (right) or expressed genes minus DEG (left). Percentage of alignment is shown in each category. (B) The frequency of genes associated with PU.1 binding. The highest percentage of genes with PU.1 peaks was in the DEG category, across WT, PU.1$^{155-/155-}$, and miR-155$^{-/-}$ B cells, at 28%. This compares with a percentage of 21% in genes with no change in expression and 12% in genes that are not expressed. The percentage of genes with PU.1 peaks relative to the total genes in each category was calculated and presented. $P < 0.001$, Chi^2 test. (C) A group of PU.1-regulated genes with links to humoral immune responses. The groups of genes with different known functions were discovered by IPA Ingenuity analysis using the genes that were differentially regulated and containing a PU.1-binding peak. Genes that contain Ig domains are colored in red. PU.1 target genes are functionally

as transcriptionally regulated by PU.1 are also expressed in macrophages and/or dendritic cells, which is consistent with the known functions of PU.1 in regulating the transcriptome of myeloid cells. Some of the genes we identified have previously been reported as PU.1 direct targets (*Cd80*, *Flt3*, *FcgrIIb*, *FcgrIV*, *Il1r1*, *Dap12*, and *Lmo2*). Overall, our analysis points toward PU.1 regulating the expression of a significant number of adhesion molecules, some of which have defined roles in cellular interactions required for productive T cell–dependent responses.

The PU.1–miR-155 interaction alone explains a large fraction of the miR-155–induced gene expression changes in activated B cells

A Venn diagram showing the distribution of the DEGs in PU.1$^{155-/155-}$ and miR-155$^{-/-}$ relative to WT allows visual inspection of the gene expression similarities (Fig. 7 A). In the PU.1$^{155-/155-}$ B cells, we found 217 up-regulated genes and 46 down-regulated genes relative to WT levels, indicating that miRNA regulation of this single target shapes the transcriptional program of B cells. Of those genes, 62% (134) of those up-regulated and 87% (40) of those down-regulated were shared with miR-155$^{-/-}$ B cells (Fig. 7 A). This number of genes is a significant component of the differentially regulated genes in miR-155$^{-/-}$ B cells, as they represent 50% of the up-regulated and 33% of the down-regulated genes. The strong overlap of the transcriptomes of PU.1$^{155-/155-}$ and miR-155$^{-/-}$ B cells suggests that PU.1 plays an important role in the gene expression changes imparted by miR-155. As reported before, a large fraction of the genes up-regulated in miR-155$^{-/-}$ B cells is enriched with miR-155 responding elements in their 3′UTRs, but the same is not observed in the down-regulated genes (Fig. 7 B; Rodriguez et al., 2007). The genes exhibiting enrichment of miR-155–binding motifs are dominated by the group of genes up-regulated in miR-155 only (Fig. 7, B and C), in line with previous studies showing that miR-155 in B cells directly regulates tens of genes in addition to PU.1 (Vigorito et al., 2007; Fabani et al., 2010). Interestingly, the fold-change in expression of DEGs relative to WT levels was generally higher in miR-155$^{-/-}$ than in PU.1$^{155-/155-}$ B cells (Table S1 and not depicted), despite the two types expressing similar levels of PU.1. This suggests that (some of) the additional miR-155 targets may act cooperatively with PU.1. When we sorted DEGs, which are PU.1 targets into those with (i) similar expression in miR-1555$^{-/-}$ and PU.1$^{155-/155-}$ or (ii) higher expression in miR-155$^{-/-}$ versus PU.1$^{155-/155-}$, GO analysis showed enrichment in different but complementary classes. Both groups are enriched in adhesion molecules and activation/differentiation molecules. Collectively these results indicate that a large component of the transcriptome changes seen in miR-155$^{-/-}$ B cells relative to WT are mediated through a single target, namely PU.1.

DISCUSSION

It is well accepted that miRNAs have had a profound impact on the evolution of 3′ UTRs and that a single miRNA can regulate the expression of hundreds of genes, although the level of repression imparted to a given target is generally low (Stark et al., 2005; Bartel, 2009). What is less evident is how the selective pressure for a single miRNA–target interaction is maintained across long evolutionary distances when the direct effect of disrupting such an interaction is apparently negligible. Here, we have shown that the miR-155/PU.1 interaction, which regulates PU.1 abundance only modestly, is key to promoting an optimal T cell–dependent extrafollicular B cell response—a previously unrecognized role for PU.1. In terms of mechanism, we have shown that, in activated B cells, PU.1 sustains Pax5 expression, acting as a negative regulator of terminal B cell differentiation. In addition to Pax5, targets of PU.1 in activated B cells include proteins involved in adhesion and cellular interactions, with direct links to B–T cell interactions. The identification of these genes provides important insights into the function of PU.1 in activated B cells.

It has been proposed that some miRNA target genes may act as bona fide targets in a particular cell type or cellular context but as miRNA-sequestering targets in other circumstances (Seitz, 2009). These alternate functions of a particular target are probably dictated by the relative abundances of the mRNA and miRNA. In this regard, it has recently been shown that a given target mRNA displays an expression threshold below which it is repressed by a miRNA but above which it titrates out the miRNA with minimal effect on protein levels (Mukherji et al., 2011). The down-regulation of PU.1 in activated B cells concomitant with the up-regulation of miR-155 provides a window of effective miRNA/target repression. This effect was very clearly observed in cultured B cells and in the context of the extrafollicular response in vivo. We propose that conserved miR–target interactions confer effectiveness to particular biological processes in a specific time window, and that in those circumstances disruption of such interactions will have measurable effects.

Our study also shows that a single target can shape significantly the overall expression program directed by a miRNA, even

enriched in those that encode adhesion molecules that regulate Ig secretion. Ingenuity Pathway Analysis (right) was performed using genes that were differentially expressed and contain PU.1 binding peak(s). A summary of the most statistically significant pathways with their P values is shown. (D) Seqmonk browser tracks of PU.1 binding at the locus of some of the genes reported to have a role in humoral immunity. WT, PU.1$^{155-/155-}$, and miR-155$^{-/-}$ B cell samples are represented, with input shown as background. Green boxes highlight the binding peak/s observed. (E) The mRNA expression of PU.1 target genes with reported roles in humoral immunity. Expression values are normalized RPKM, determined from 4 to 5 biological replicates in each of the genotypes or AU for q-PCR measured from 3 experiments with 3–4 mice per group. Statistical analysis was assessed with one-way ANOVA test. *, $P < 0.05$; **, $P < 0.001$; ***, $P < 0.0001$. Data analysis in A–D is based on one experiment with 4–5 biological replicates per genotype.

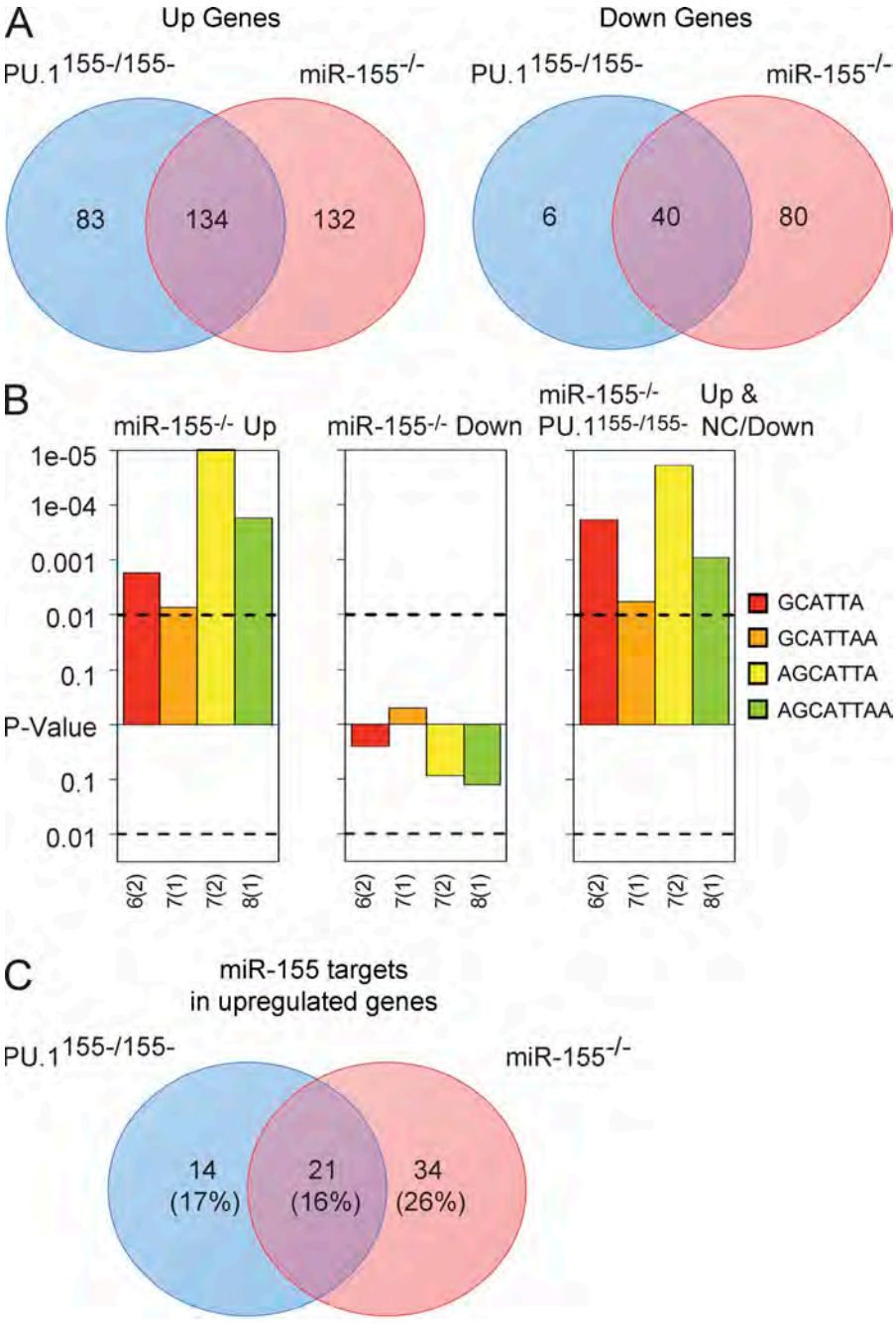

Figure 7. PU.1 explains a large fraction of changes in the transcriptome of miR-155–deficient B cells. (A) Venn diagrams intersecting the number of genes up-regulated or down-regulated in PU.1$^{155-/155-}$, or miR-155$^{-/-}$ samples, compared with WT. All genes tested are from the DEG group of genes listed in Table S1. (B) Sylamer analysis for genes either up- or down-regulated in miR-155$^{-/-}$ compared with WT, for enrichment of miR-155–binding sites (6-mer, 7-mer, or 8-mer composition). Also tested were genes up-regulated in miR-155$^{-/-}$ but down-regulated or without change in expression in PU.1$^{155-/155-}$ samples. Significance was calculated by comparing enrichment of the miR-155 seed sequence in these selected groups of genes to all the genes containing a 3′UTR in the mouse genome. (C) Venn diagram intersecting the number of genes with miR-155–binding sites in PU.1$^{155-/155-}$ or miR-155$^{-/-}$ up-regulated genes. Percentages in brackets represent the number of genes with miR-155–binding sites as a proportion of the total number of up-regulated genes.

though the miRNA has many additional targets, as indicated by the extensive overlap in the transcriptomes of PU.1$^{155-/155-}$ and miR-155$^{-/-}$-activated B cells. Despite the strong impact of PU.1 on miR-155 regulation of gene expression, we consistently observed that the fold-change in expression of DEGs relative to WT levels was higher in miR-155$^{-/-}$ than in PU.1$^{155-/155-}$ B cells. In other words, most of the DEGs in PU.1$^{155-/155-}$ B cells show intermediate expression relative to WT and miR-155$^{-/-}$. This is also manifested in the impaired Ig production in vivo, which is more severe in the miR-155$^{-/-}$ mice. At present we do not know the basis of this phenomenon but suggest that synergy with additional miR-155 targets may be occurring. It is likely that an answer to this will emerge from the analysis of in vivo activated B cells from PU.1$^{155-/155-}$ and miR-155$^{-/-}$ mice and this is an area that requires further investigation.

It is well recognized that effective transitions through developmental programs require strict control of the abundance of regulatory components. Posttranscriptional control of gene expression by miRNAs provides an effective mechanism to ensure timely transitions across developmental stages. In fact, dose-sensitive genes that regulate B cell activation in vivo, such as *Irf4*, *Bcl6*, *Aicda*, or *Prdm1,* are susceptible to miRNA regulation (de Yébenes et al., 2008; Teng et al., 2008; Malumbres

et al., 2009; West et al., 2009; Gururajan et al., 2010; Borchert et al., 2011; Chaudhuri et al., 2011; Lin et al., 2011; Huang et al., 2012). Although the significance of some of the aforementioned posttranscriptional regulation events remains to be explored in vivo, the interplay between transcription factors and miRNAs is emerging as a common theme in gene regulatory networks (Le et al., 2013). We show here that regulation of PU.1 abundance by miR-155 in activated B cells impacts on terminal B cell differentiation in vivo and in vitro. The increased expression of PU.1, due to lack of miR-155 regulation, results in higher levels of Pax5 and lower levels of Blimp-1 concomitant with a reduction of plasma cells. Moreover, we were able to restore plasma cell differentiation in miR-155$^{-/-}$ and PU.1$^{155-/155-}$ B cells by simply reducing Pax5 expression. In agreement with our results, sustained ectopic expression of Pax5 in murine splenocytes activated with LPS has been shown to inhibit plasma cell formation (Lin et al., 2002). In agreement with our results, Carotta et al. (this issue) have observed that overexpression or reduction of PU.1 expression in mature B cells affected Pax-5 and Blimp1 expression, suggesting a role for PU.1 as a negative regulator of plasma cell differentiation. Therefore, we propose that miR-155 regulates the initiation of the plasma cell differentiation pathway through the inhibition of PU.1, which in turn regulates the expression of Pax5.

Genome-wide characterization of genes regulated transcriptionally by PU.1 shows that several of them encode membrane receptors with roles in cellular adhesion and intercellular communication. This functional pattern is consistent with previous reports mainly focused on myeloid cells (Turkistany and DeKoter, 2011), suggesting a broader role for PU.1 in the regulation of antigen-presenting function in myeloid and B cells. Among the genes regulated by PU.1 are Plexin-d1, semaphorin family members, and Dap12, which can act as an adaptor for Plexin-d1. Plexin-d1 plays a B cell–intrinsic role in T cell–dependent responses, probably by regulating B cell migration within germinal centers (Yu et al., 2008; Holl et al., 2011). In addition to the already characterized PU.1 target FcgRIIb, Fcgr3a and Fcrl5 also appear to be direct targets of PU.1. Although there is still controversy over the identity of the ligand for Fcrl5, it is clear it can provide inhibitory signals to human B cells (Haga et al., 2007), which may contribute to explaining the inhibitory role of PU.1 in activated B cells. A group of target genes (*IcosL*, *PD1lg2*, *Pvrl1 [Nectin-1]*, and *Slamf1*) with well-defined roles in T follicular helper cell interactions has been identified. With the exception of the negative regulator *PD1lg2*, these genes appear to be activated transcriptionally by PU.1, and hence promote stronger interactions with T follicular helper cells: the possibility that collective changes in the expression of these genes could impact on intercellular communication in activated B cells remains to be tested. A theme on the regulation of T cell interactions is also suggested by PU.1 regulating Alcam and CD80, the latter already described as a target of PU.1 (Bowen et al., 1995; Kanada et al., 2011). Both Alcam and CD80 are known to be expressed by activated B cells (Bowen et al., 1995). Alcam regulates T cell function via binding of its ligand CD6 that appears to have inhibitory signaling function (Oliveira et al., 2012), whereas CD80 preferentially recruits the inhibitory molecule CTLA-4 to the T cell immunological synapse and may as a consequence inhibit T cell activation (Pentcheva-Hoang et al., 2004). Additional PU.1 targets include Sirpa and Adora, both of which regulate T cell activation and effector function; however, their roles in B cells have yet to be studied. Overall, our results establish a novel negative regulatory function for PU.1 in activated B cells and identify a wide set of targets. In addition to Pax5 we have uncovered a set of genes with roles in cell adhesion and cellular communication that may regulate B–T cell interaction to mediate effective immune responses. Our study also highlights the need to manipulate miRNA–target interactions in physiological settings to advance our understanding on miRNA biology. It is only in this way that we can formally establish cause–effect relationships and distinguish epistasis between miRNAs and their targets.

MATERIALS AND METHODS

Mice. miR-155 mice, described previously (Rodriguez et al., 2007), were backcrossed six times to C57BL/6J. C57BL/6J mice were obtained from The Jackson Laboratory and were bred at the Babraham Institute. PU.1$^{155-/155-}$ mice were generated at the Babraham Institute (details below). All animal experimentation complied with UK Home Office regulations and was approved by the local ethical review process at The Babraham Research Campus.

Generation of PU.1$^{155-/155-}$ mice and chimeras. The PU.1$^{155-/155-}$ targeting construct was derived from a previously described PU.1 knock-out targeting vector (Dakic et al., 2005). In brief, a fragment of 1.1-kb flanking the miR-155–binding site in the 3′UTR of PU.1 was cleaved from the targeting vector using the restriction enzyme SalI. This was cloned into pBluescript SK in which site direct mutagenesis was performed using the Quick Change Multi Site kit (Agilent Technologies) with the following primers: 5′-GACCCCGCCGGCCATAGATGCATCCCGTCGCCCGGCCCGG-3′ and 5′-CCGGGCCGGGCGACGGGATGCATCTATGGCCGGCGGG-GTC-3′. The nucleotides underlined indicate those mutated. The mutation introduces an NsiI restriction site, which was used for genotyping purposes. Once the mutation had been sequence verified, the mutated fragment was cloned back into the targeting vector using the same SalI restriction site and checked for correct orientation by restriction profile and sequencing. The linear targeting vector was transfected into C57BL/6 ES cells. Neomycin-resistant clones were screened by Southern hybridization and chimeras derived from blastocyst injection of these targeted clones were crossed to obtain germline transmission. FLPe mice were then crossed with the PU.1$^{155/GFP}$ mice for the removal of the IRES-GFP-Neomycin cassette and to obtain PU.1$^{155-/+}$ mice. Further breeding produced the PU.1$^{155-/155-}$ homozygous mice used in this study. For the generation of mixed chimeras, 500-rads irradiated μMT mice received 5×10^6 of a mixture of 80% bone marrow cells of μMT origin and 20% WT, PU.1$^{155-/155-}$, or miR-155–deficient bone marrow cells. Reconstitution was assessed 6 wk later by measuring B and T cells from blood.

Luciferase assay. The *Sfpi1* 3′UTR was amplified from genomic DNA and inserted into the psiCheck-2 Renilla luciferase reporter plasmid (Promega, (Vigorito et al., 2007)). This construct was used to derive a miR-155 "seed" mutant plasmid with the Quik Change Multi Site Mutagenesis kit (Agilent Technologies). The mutagenic primers used were the same reported in the previous section to generate the knock-in mice. The correctness of all plasmids was confirmed by sequencing. Reporter assays were performed in

HeLa cells co-transfected in triplicates using Lipofectamine 2000 (Invitrogen) with test plasmid (3′UTR PU.1 WT or mutant) along with the indicated mimic at a final concentration of 40 nM. Firefly luciferase was used as a normalization control. Reporter activity was detected 24 h after transfection with the Dual-Glo Luciferase Assay System (Promega). Expression values were normalized against the average value for the corresponding plasmid as in (Rodriguez et al., 2007).

Immunization, ELISA, and ELISPOT. To elicit a T cell–dependent immune response, 100 µg of alum-precipitated NP-KLH (Biosearch Tech) was used. NP-specific antibodies were detected by ELISA, as previously described (Vigorito et al., 2007), except that antibody end point titers were used as a measurement of relative concentration. NP-specific AFCs were detected with ELISPOT as previously described (Xiang et al., 2007). In brief, 96-well plates (Millipore) were coated with NP_{23}-BSA and blocked with 10% FCS in medium before the addition of splenic cells. Cells were incubated overnight under 5% CO_2 at 37°C in complete medium (see Cell culture and FACS analysis). Cells secreting anti-NP antibody were visualized with HRP anti–mouse IgM or IgG1 followed by ACE staining (Sigma-Aldrich).

RNA extraction and qPCR. Total RNA was extracted using TRIzol (Invitrogen) according to the manufacturer's protocol. cDNA synthesis was performed using Superscript III (Invitrogen). qPCR analysis was performed using the SYBR Green JumpStart Taq ReadyMix (Sigma-Aldrich). A list of the primers used is shown in Table S2. Cycling conditions were as follows: Step 1, 2 min at 95°C; Step 2, 15 s at 95°C; Step 3, 30 s at 65°C; Step 4, 30 s at 72°C. Steps 2–4 were repeated for 40 cycles. Data acquired were analyzed using the software supplied by the manufacture (Bio-Rad Laboratories). Relative quantifications of gene expression were calculated using either Hprt or β-actin as control. miR-155 was quantified using a TaqMan assay and U6 as control according to manufacturer's instructions. In the Pax5 ChIP qPCR, primers amplifying a region in the enhancer element in intron 5 were applied to DNA fragments immunoprecipitated using an anti-PU.1 antibody (Santa Cruz Biotechnology, Inc.) and normalized against β-actin. In the sorted GFP^+ retrovirally transfected cells, the QuantiTect SYBR Green RT-PCR system was used (QIAGEN).

Western blotting. Western blots were performed on cell lysates prepared using 100 µl of RIPA buffer, consisting of 150 mM NaCl, 50 mM Tris-HCl pH 8, 1% NP-40, 0.5% deoxycholate, and 0.1% SDS per 10^7 stimulated splenocytes. Protein concentration was measured using a BCA assay (Thermo Fisher Scientific) and 50 µg of protein lysate were loaded per lane onto an 8% SDS-PAGE gel. After electrophoresis, the separated polypeptides were transferred to a nitrocellulose membrane and immunostained using a rabbit anti-PU.1 antibody (Santa Cruz Biotechnology, Inc.), anti-Pax5 (Holmes et al., 2006), or mouse anti-tubulin (Sigma-Aldrich) primary antibodies. IRDye 800 anti–rabbit IgG and Alexa Fluor 680 anti–mouse IgG (Invitrogen) were used for development and imaging. Blot images were analyzed on a Li-COR Odyssey system.

Cell culture and FACS sorting. Lymphocytes were isolated from the spleen of mice by density gradient separation using Lympholyte-M (Cedarlane). B cells were further purified using a negative selection B cell isolation kit (Miltenyi Biotec). Cells were cultured in RPMI-1640 (Invitrogen) containing 10% FCS, 2 mM L-glutamine, 2-mercaptoethanol, and 1% penicillin/streptomycin. To monitor proliferation, up to 10^7 cells were labeled with 25 µM CFSE for 10 min to track cell division. Cells were stimulated with 5 µg/ml LPS (Sigma-Aldrich) and 10 ng/ml of IL-4 (PeproTech). Cells were surface-stained with antibodies listed in Table S2 and with DAPI (Invitrogen) for exclusion of dead cells. For Pax5 intracellular staining, the cells were fixed with the Foxp3 staining buffer set (eBioscience) according to manufacturer's instructions. Data were acquired in a LSRFortessa or LSRII (BD) and analyzed on FlowJo (Tree Star). All cell sorting was performed on a FACSAria III instrument (BD).

RNAi gene silencing assay. The target sequence was introduced into the pMig empty retroviral vector via the BLOCK-iT polII miR RNAi vector kit (Invitrogen). The vectors were sequence confirmed before being introduced into the Plat-E retroviral packaging system with the X-treme GENE HP DNA transfection reagent (Roche). Retroviral supernatants were treated with PEG-iT virus precipitation solution (System Biosciences) for 12 h before centrifuged for 30 min at 500 *g*. All retroviral vectors expressed GFP, and an empty retroviral vector containing GFP only was used as the control.

Chromatin immunoprecipitation. Cultured B cells stimulated for 4 d with LPS (5 µg/ml) and IL-4 (10 ng/ml) were treated with 2% formaldehyde to cross-link the DNA and protein and incubated for 5 min at room temperature. This reaction was quenched by adding glycine to a final concentration of 125 mM. Cells were then permeabilized in 5 mM PIPES, pH 8.0, 85 mM KCl, 0.5% NP-40, and protease inhibitor cocktail (Roche) for 15 min at 4°C. Lysis buffer consisting of 1% SDS, 10 mM EDTA, and 50 mM Tris-HCl was applied to the permeabilized cells before fragmentation using a Diagenode Bioraptor UCD-200 sonicator.

Fragmented chromatin was diluted to 50 µg/ml in ChIP buffer, containing 0.01% SDS, 1.1% Triton-100, 1.2 mM EDTA, 16.7 mM Tris-HCl, 167 mM NaCl, and protease inhibitors cocktail (Roche). 1 ml was used per immunoprecipitation reaction and 100 µl was used as input control. The chromatin was incubated with either 2.0 µg of rabbit α-PU.1 (T-21 clone; Santa Cruz Biotechnology, Inc.) or the same amount of IgG isotype control overnight and precipitated using 50 µl protein A-coated magnetic beads (Invitrogen). Precipitates were then reverse cross-linked, mRNA and proteins were digested using RNase A and proteinase K by incubating at 37 °C for 1 h and at 65°C overnight. After phenol/chloroform extraction, DNA was precipitated using isopropanol and resuspended in TE.

Library preparation for ChIP-Seq and RNA-Seq. ChIP-Seq libraries were constructed essentially following Illumina's standard ChIP-Seq library construction protocols. RNA-Seq libraries were constructed using the TruSeq sample preparation kit (Illumina) except that after the first strand synthesis, the reaction mixture was cleaned up using the QIAQuick purification columns (QIAGEN) and the second strand synthesis was made using dUTP instead of dTTP. Just before the PCR amplification step, UNG (Ambion) was used to digest the second (opposite) strand containing uracil, to make it strand-specific. Both ChIP and RNA libraries were run on the Bioanalyzer for quality control to check purity and size range.

Sequencing and read alignment. ChIP-Seq was performed on the Illumina Genome Analyser IIx using the 36-bp read length program. RNA-seq was performed on the Hi-Seq 2000 using the 75-bp read length program. The barcoded samples were then de-multiplexed and mapping was performed with the NCBIM37 (mm9) reference genome using Bowtie for ChIP-Seq and TopHat for RNA-Seq, respectively.

Peak calling and motif analysis for ChIP-seq. ChIP-Seq peaks were called using the default parameters on the MACS software version 1.3.6.1 (Zhang et al., 2008) and viewed using the SeqMonk program. For PU.1 motif discovery, the center 200 bp of called peaks were analyzed using the MEME suite program (Bailey et al., 2009) for alignment. For cis-regulatory motif analysis, the same sequences used in the MEME program were run in the RSAT pattern matching program using predefined motifs (Heinz et al., 2010). For PU.1 motif discovery, the center 200 bp of called peaks were analyzed using the MEME suite program (Bailey et al., 2009) for alignment.

Transcriptome annotation and quantification. To determine whether a given gene is defined as "expressed," an initial quantitation was made by counting the number of RPKM, where the normal distribution was viewed and an expression cut-off of RPKM=1 was chosen. To identify significantly changing genes, RPM values were quantitated. Differential expression was called by selecting transcripts, which changed with a significance of $P < 0.05$ after Benjamini and Hochberg correction using a null model constructed

from the 0.1% of transcripts showing the closest average level of observation to estimate experimental noise.

Accession numbers. All sequencing data discussed in this paper are available at the Gene Expression Omnibus (GEO) repository at NCBI under the number GSE61426.

Pathway analysis. Functional enrichment analysis (GO analysis) was performed using the DEG list that also had PU.1 binding assigned into the DAVID web tool. For IPA Ingenuity pathway analysis, the expression values of the above gene list were also used in performing the pathway search.

Statistical analysis. Data are presented as mean ± SEM or SD as indicated in the figures. Mean comparisons between groups were performed using a two-sided one-way ANOVA test. A p-value <0.05 was taken as statistically significant. *, $P < 0.05$; **, $P < 0.01$; ***, $P < 0.001$. In Fig. 6 B, a χ^2 test was performed.

Online supplemental material. Table S1 contains data combining ChIP-Seq and RNA-Seq data. Table S2 provides a list of primers and FACS antibodies. Online supplemental material is available at http://www.jem.org/cgi/content/full/jem.20140338/DC1.

We thank the staff of the Babraham Institute small animal facility for mouse husbandry, Geoff Morgan and Arthur Davis for support with FACS analysis, Ted Saunders and Martin George for ES cell and blastocyst manipulation, Michelle Linterman for helpful discussions and a critical reading of the manuscript.

This work was supported by the Medical Research Council through a CDA fellowship (G0700287) and grant (G1001781) to EV as well as funding from the BBSRC. SLN is supported by an Australian Research Council Future Fellowship. This work was made possible through Victorian State Government Operational Infrastructure Support and Australian Government NHMRC IRIIS.

The authors declare no additional competing financial interests.

Submitted: 19 February 2014
Accepted: 18 August 2014

REFERENCES

Bailey, T.L., M. Boden, F.A. Buske, M. Frith, C.E. Grant, L. Clementi, J. Ren, W.W. Li, and W.S. Noble. 2009. MEME SUITE: tools for motif discovery and searching. *Nucleic Acids Res.* 37:W202-W208. http://dx.doi.org/10.1093/nar/gkp335

Bartel, D.P. 2009. MicroRNAs: target recognition and regulatory functions. *Cell*. 136:215–233. http://dx.doi.org/10.1016/j.cell.2009.01.002

Belver, L., F.N. Papavasiliou, and A.R. Ramiro. 2011. MicroRNA control of lymphocyte differentiation and function. *Curr. Opin. Immunol.* 23:368–373. http://dx.doi.org/10.1016/j.coi.2011.02.001

Berger, A.H., and P.P. Pandolfi. 2011. Haplo-insufficiency: a driving force in cancer. *J. Pathol.* 223:137–146. http://dx.doi.org/10.1002/path.2800

Borchert, G.M., N.W. Holton, and E.D. Larson. 2011. Repression of human activation induced cytidine deaminase by miR-93 and miR-155. *BMC Cancer.* 11:347. http://dx.doi.org/10.1186/1471-2407-11-347

Bowen, M.A., D.D. Patel, X. Li, B. Modrell, A.R. Malacko, W.C. Wang, H. Marquardt, M. Neubauer, J.M. Pesando, U. Francke, et al. 1995. Cloning, mapping, and characterization of activated leukocyte-cell adhesion molecule (ALCAM), a CD6 ligand. *J. Exp. Med.* 181:2213–2220. http://dx.doi.org/10.1084/jem.181.6.2213

Carotta, S., A. Dakic, A. D'Amico, S.H.M. Pang, K.T. Greig, S.L. Nutt, and L. Wu. 2010a. The transcription factor PU.1 controls dendritic cell development and Flt3 cytokine receptor expression in a dose-dependent manner. *Immunity*. 32:628–641. http://dx.doi.org/10.1016/j.immuni.2010.05.005

Carotta, S., L. Wu, and S.L. Nutt. 2010b. Surprising new roles for PU.1 in the adaptive immune response. *Immunol. Rev.* 238:63–75. http://dx.doi.org/10.1111/j.1600-065X.2010.00955.x

Chaudhuri, A.A., A.Y.-L. So, N. Sinha, W.S.J. Gibson, K.D. Taganov, R.M. O'Connell, and D. Baltimore. 2011. MicroRNA-125b potentiates macrophage activation. *J. Immunol.* 187:5062–5068. http://dx.doi.org/10.4049/jimmunol.1102001

Dakic, A., D. Metcalf, L. Di Rago, S. Mifsud, L. Wu, and S.L. Nutt. 2005. PU.1 regulates the commitment of adult hematopoietic progenitors and restricts granulopoiesis. *J. Exp. Med.* 201:1487–1502. http://dx.doi.org/10.1084/jem.20050075

de Yébenes, V.G., L. Belver, D.G. Pisano, S. González, A. Villasante, C. Croce, L. He, and A.R. Ramiro. 2008. miR-181b negatively regulates activation-induced cytidine deaminase in B cells. *J. Exp. Med.* 205:2199–2206. http://dx.doi.org/10.1084/jem.20080579

Decker, T., M. Pasca di Magliano, S. McManus, Q. Sun, C. Bonifer, H. Tagoh, and M. Busslinger. 2009. Stepwise activation of enhancer and promoter regions of the B cell commitment gene Pax5 in early lymphopoiesis. *Immunity*. 30:508–520. http://dx.doi.org/10.1016/j.immuni.2009.01.012

Dorsett, Y., K.M. McBride, M. Jankovic, A. Gazumyan, T.-H. Thai, D.F. Robbiani, M. Di Virgilio, B. Reina San-Martin, G. Heidkamp, T.A. Schwickert, et al. 2008. MicroRNA-155 suppresses activation-induced cytidine deaminase-mediated Myc-Igh translocation. *Immunity*. 28:630–638. http://dx.doi.org/10.1016/j.immuni.2008.04.002

Fabani, M.M., C. Abreu-Goodger, D. Williams, P.A. Lyons, A.G. Torres, K.G.C. Smith, A.J. Enright, M.J. Gait, and E. Vigorito. 2010. Efficient inhibition of miR-155 function in vivo by peptide nucleic acids. *Nucleic Acids Res.* 38:4466–4475. http://dx.doi.org/10.1093/nar/gkq160

Fisher, E., and P. Scambler. 1994. Human haploinsufficiency—one for sorrow, two for joy. *Nat. Genet.* 7:5–7. http://dx.doi.org/10.1038/ng0594-5

Friedman, R.C., K.K.-H. Farh, C.B. Burge, and D.P. Bartel. 2009. Most mammalian mRNAs are conserved targets of microRNAs. *Genome Res.* 19:92–105. http://dx.doi.org/10.1101/gr.082701.108

Gururajan, M., C.L. Haga, S. Das, C.-M. Leu, D. Hodson, S. Josson, M. Turner, and M.D. Cooper. 2010. MicroRNA 125b inhibition of B cell differentiation in germinal centers. *Int. Immunol.* 22:583–592. http://dx.doi.org/10.1093/intimm/dxq042

Haga, C.L., G.R.A. Ehrhardt, R.J. Boohaker, R.S. Davis, and M.D. Cooper. 2007. Fc receptor-like 5 inhibits B cell activation via SHP-1 tyrosine phosphatase recruitment. *Proc. Natl. Acad. Sci. USA*. 104:9770–9775. http://dx.doi.org/10.1073/pnas.0703354104

Hasbold, J., L.M. Corcoran, D.M. Tarlinton, S.G. Tangye, and P.D. Hodgkin. 2004. Evidence from the generation of immunoglobulin G-secreting cells that stochastic mechanisms regulate lymphocyte differentiation. *Nat. Immunol.* 5:55–63. http://dx.doi.org/10.1038/ni1016

Heinz, S., C. Benner, N. Spann, E. Bertolino, Y.C. Lin, P. Laslo, J.X. Cheng, C. Murre, H. Singh, and C.K. Glass. 2010. Simple combinations of lineage-determining transcription factors prime cis-regulatory elements required for macrophage and B cell identities. *Mol. Cell.* 38:576–589. http://dx.doi.org/10.1016/j.molcel.2010.05.004

Ho, F., J.E. Lortan, I.C. MacLennan, and M. Khan. 1986. Distinct short-lived and long-lived antibody-producing cell populations. *Eur. J. Immunol.* 16:1297–1301. http://dx.doi.org/10.1002/eji.1830161018

Holl, E.K., B.P. O'Connor, T.M. Holl, K.E. Roney, A.G. Zimmermann, S. Jha, G. Kelsoe, and J.P.-Y. Ting. 2011. Plexin-D1 is a novel regulator of germinal centers and humoral immune responses. *J. Immunol.* 186:5603–5611. http://dx.doi.org/10.4049/jimmunol.1003464

Holmes, M.L., S. Carotta, L.M. Corcoran, and S.L. Nutt. 2006. Repression of Flt3 by Pax5 is crucial for B-cell lineage commitment. *Genes Dev.* 20:933–938. http://dx.doi.org/10.1101/gad.1396206.

Houston, I.B., M.B. Kamath, B.L. Schweitzer, T.M. Chlon, and R.P. DeKoter. 2007. Reduction in PU.1 activity results in a block to B-cell development, abnormal myeloid proliferation, and neonatal lethality. *Exp. Hematol.* 35:1056–1068. http://dx.doi.org/10.1016/j.exphem.2007.04.005

Huang, X., X. Zhou, Z. Wang, F. Li, F. Liu, L. Zhong, X. Li, X. Han, Z. Wu, S. Chen, and T. Zhao. 2012. CD99 triggers upregulation of miR-9-modulated PRDM1/BLIMP1 in Hodgkin/Reed-Sternberg cells and induces redifferentiation. *Int. J. Cancer.* 131:E382–E394. http://dx.doi.org/10.1002/ijc.26503

Iwasaki, H., C. Somoza, H. Shigematsu, E.A. Duprez, J. Iwasaki-Arai, S. Mizuno, Y. Arinobu, K. Geary, P. Zhang, T. Dayaram, et al. 2005. Distinctive and indispensable roles of PU.1 in maintenance of hematopoietic stem cells and

their differentiation. *Blood*. 106:1590–1600. http://dx.doi.org/10.1182/blood-2005-03-0860

Jacob, J., R. Kassir, and G. Kelsoe. 1991a. In situ studies of the primary immune response to (4-hydroxy-3-nitrophenyl)acetyl. I. The architecture and dynamics of responding cell populations. *J. Exp. Med*. 173:1165–1175. http://dx.doi.org/10.1084/jem.173.5.1165

Jacob, J., G. Kelsoe, K. Rajewsky, and U. Weiss. 1991b. Intraclonal generation of antibody mutants in germinal centres. *Nature*. 354:389–392. http://dx.doi.org/10.1038/354389a0

Kallies, A., J. Hasbold, K. Fairfax, C. Pridans, D. Emslie, B.S. McKenzie, A.M. Lew, L.M. Corcoran, P.D. Hodgkin, D.M. Tarlinton, and S.L. Nutt. 2007. Initiation of plasma-cell differentiation is independent of the transcription factor Blimp-1. *Immunity*. 26:555–566. http://dx.doi.org/10.1016/j.immuni.2007.04.007

Kanada, S., C. Nishiyama, N. Nakano, R. Suzuki, K. Maeda, M. Hara, N. Kitamura, H. Ogawa, and K. Okumura. 2011. Critical role of transcription factor PU.1 in the expression of CD80 and CD86 on dendritic cells. *Blood*. 117:2211–2222. http://dx.doi.org/10.1182/blood-2010-06-291898

Laslo, P., C.J. Spooner, A. Warmflash, D.W. Lancki, H.-J. Lee, R. Sciammas, B.N. Gantner, A.R. Dinner, and H. Singh. 2006. Multilineage transcriptional priming and determination of alternate hematopoietic cell fates. *Cell*. 126:755–766. http://dx.doi.org/10.1016/j.cell.2006.06.052

Le, T.D., L. Liu, B. Liu, A. Tsykin, G.J. Goodall, K. Satou, and J. Li. 2013. Inferring microRNA and transcription factor regulatory networks in heterogeneous data. *BMC Bioinformatics*. 14:92. http://dx.doi.org/10.1186/1471-2105-14-92

Lin, K.-I., C. Angelin-Duclos, T.C. Kuo, and K. Calame. 2002. Blimp-1-dependent repression of Pax-5 is required for differentiation of B cells to immunoglobulin M-secreting plasma cells. *Mol. Cell. Biol*. 22:4771–4780. http://dx.doi.org/10.1128/MCB.22.13.4771-4780.2002

Lin, J., T. Lwin, J.-J. Zhao, W. Tam, Y.S. Choi, L.C. Moscinski, W.S. Dalton, E.M. Sotomayor, K.L. Wright, and J. Tao. 2011. Follicular dendritic cell-induced microRNA-mediated upregulation of PRDM1 and downregulation of BCL-6 in non-Hodgkin's B-cell lymphomas. *Leukemia*. 25:145–152. http://dx.doi.org/10.1038/leu.2010.230

Linterman, M.A., R.J. Rigby, R.K. Wong, D. Yu, R. Brink, J.L. Cannons, P.L. Schwartzberg, M.C. Cook, G.D. Walters, and C.G. Vinuesa. 2009. Follicular helper T cells are required for systemic autoimmunity. *J. Exp. Med*. 206:561–576. http://dx.doi.org/10.1084/jem.20081886

Liu, Y.J., J. Zhang, P.J. Lane, E.Y. Chan, and I.C. MacLennan. 1991. Sites of specific B cell activation in primary and secondary responses to T cell-dependent and T cell-independent antigens. *Eur. J. Immunol*. 21:2951–2962. http://dx.doi.org/10.1002/eji.1830211209

MacLennan, I.C.M., K.-M. Toellner, A.F. Cunningham, K. Serre, D.M.-Y. Sze, E. Zúñiga, M.C. Cook, and C.G. Vinuesa. 2003. Extrafollicular antibody responses. *Immunol. Rev*. 194:8–18. http://dx.doi.org/10.1034/j.1600-065X.2003.00058.x

Malumbres, R., K.A. Sarosiek, E. Cubedo, J.W. Ruiz, X. Jiang, R.D. Gascoyne, R. Tibshirani, and I.S. Lossos. 2009. Differentiation stage-specific expression of microRNAs in B lymphocytes and diffuse large B-cell lymphomas. *Blood*. 113:3754–3764. http://dx.doi.org/10.1182/blood-2008-10-184077

Martins, G., and K. Calame. 2008. Regulation and functions of Blimp-1 in TandBlymphocytes. *Annu. Rev. Immunol*. 26:133–169. http://dx.doi.org/10.1146/annurev.immunol.26.021607.090241

Mukherji, S., M.S. Ebert, G.X.Y. Zheng, J.S. Tsang, P.A. Sharp, and A. van Oudenaarden. 2011. MicroRNAs can generate thresholds in target gene expression. *Nat. Genet*. 43:854–859. http://dx.doi.org/10.1038/ng.905

O'Connell, R.M., K.D. Taganov, M.P. Boldin, G. Cheng, and D. Baltimore. 2007. MicroRNA-155 is induced during the macrophage inflammatory response. *Proc. Natl. Acad. Sci. USA*. 104:1604–1609. http://dx.doi.org/10.1073/pnas.0610731104

Ochiai, K., M. Maienschein-Cline, G. Simonetti, J. Chen, R. Rosenthal, R. Brink, A.S. Chong, U. Klein, A.R. Dinner, H. Singh, and R. Sciammas. 2013. Transcriptional regulation of germinal center B and plasma cell fates by dynamical control of IRF4. *Immunity*. 38:918–929. http://dx.doi.org/10.1016/j.immuni.2013.04.009

Oliveira, M.I., C.M. Gonçalves, M. Pinto, S. Fabre, A.M. Santos, S.F. Lee, M.A.A. Castro, R.J. Nunes, R.R. Barbosa, J.R. Parnes, et al. 2012. CD6 attenuates early and late signaling events, setting thresholds for T-cell activation. *Eur. J. Immunol*. 42:195–205. http://dx.doi.org/10.1002/eji.201040528

Pentcheva-Hoang, T., J.G. Egen, K. Wojnoonski, and J.P. Allison. 2004. B7-1 and B7-2 selectively recruit CTLA-4 and CD28 to the immunological synapse. *Immunity*. 21:401–413. http://dx.doi.org/10.1016/j.immuni.2004.06.017

Rodriguez, A., E. Vigorito, S. Clare, M.V. Warren, P. Couttet, D.R. Soond, S. van Dongen, R.J. Grocock, P.P. Das, E.A. Miska, et al. 2007. Requirement of bic/microRNA-155 for normal immune function. *Science*. 316:608–611. http://dx.doi.org/10.1126/science.1139253

Rosenbauer, F., K. Wagner, J.L. Kutok, H. Iwasaki, M.M. Le Beau, Y. Okuno, K. Akashi, S. Fiering, and D.G. Tenen. 2004. Acute myeloid leukemia induced by graded reduction of a lineage-specific transcription factor, PU.1. *Nat. Genet*. 36:624–630. http://dx.doi.org/10.1038/ng1361

Sciammas, R., A.L. Shaffer, J.H. Schatz, H. Zhao, L.M. Staudt, and H. Singh. 2006. Graded expression of interferon regulatory factor-4 coordinates isotype switching with plasma cell differentiation. *Immunity*. 25:225–236. http://dx.doi.org/10.1016/j.immuni.2006.07.009

Seitz, H. 2009. Redefining microRNA targets. *Curr. Biol*. 19:870–873. http://dx.doi.org/10.1016/j.cub.2009.03.059

Stark, A., J. Brennecke, N. Bushati, R.B. Russell, and S.M. Cohen. 2005. Animal MicroRNAs confer robustness to gene expression and have a significant impact on 3'UTR evolution. *Cell*. 123:1133–1146. http://dx.doi.org/10.1016/j.cell.2005.11.023

Teng, G., P. Hakimpour, P. Landgraf, A. Rice, T. Tuschl, R. Casellas, and F.N. Papavasiliou. 2008. MicroRNA-155 is a negative regulator of activation-induced cytidine deaminase. *Immunity*. 28:621–629. http://dx.doi.org/10.1016/j.immuni.2008.03.015

Thai, T.H., D.P. Calado, S. Casola, K.M. Ansel, C. Xiao, Y. Xue, A. Murphy, D. Frendewey, D. Valenzuela, J.L. Kutok, et al. 2007. Regulation of the germinal center response by microRNA-155. *Science*. 316:604–608. http://dx.doi.org/10.1126/science.1141229

Turkistany, S.A., and R.P. DeKoter. 2011. The transcription factor PU.1 is a critical regulator of cellular communication in the immune system. *Arch. Immunol. Ther. Exp. (Warsz.)*. 59:431–440. http://dx.doi.org/10.1007/s00005-011-0147-9

Vigorito, E., K.L. Perks, C. Abreu-Goodger, S. Bunting, Z. Xiang, S. Kohlhaas, P.P. Das, E.A. Miska, A. Rodriguez, A. Bradley, et al. 2007. microRNA-155 regulates the generation of immunoglobulin class-switched plasma cells. *Immunity*. 27:847–859. http://dx.doi.org/10.1016/j.immuni.2007.10.009

West, J.A., S.R. Viswanathan, A. Yabuuchi, K. Cunniff, A. Takeuchi, I.-H. Park, J.E. Sero, H. Zhu, A. Perez-Atayde, A.L. Frazier, et al. 2009. A role for Lin28 in primordial germ-cell development and germ-cell malignancy. *Nature*. 460:909–913.

Yu, D., M.C. Cook, D.-M. Shin, D.G. Silva, J. Marshall, K.-M. Toellner, W.L. Havran, P. Caroni, M.P. Cooke, H.C. Morse, et al. 2008. Axon growth and guidance genes identify T-dependent germinal centre B cells. *Immunol. Cell Biol*. 86:3–14. http://dx.doi.org/10.1038/sj.icb.7100123

Xiang, Z., A.J. Cutler, R.J. Brownlie, K. Fairfax, K.E. Lawlor, E. Severinson, E.U. Walker, R.A. Manz, D.M. Tarlinton, and K.G.C. Smith. 2007. FcgammaRIIb controls bone marrow plasma cell persistence and apoptosis. *Nat. Immunol*. 8:419–429. http://dx.doi.org/10.1038/ni1440.

Zhang, Y., T. Liu, C.A. Meyer, J. Eeckhoute, D.S. Johnson, B.E. Bernstein, C. Nusbaum, R.M. Myers, M. Brown, W. Li, and X.S. Liu. 2008. Model-based analysis of ChIP-Seq (MACS). *Genome Biol*. 9:R137. http://dx.doi.org/10.1186/gb-2008-9-9-r137